

Repurposing the scientific literature with vision-language models

Anton Alyakin^{1,2,3}, Jaden Stryker¹, Daniel Alexander Alber^{1,4}, Karl L. Sangwon^{1,4}, Brandon Duderstadt⁵, Akshay Save¹, David Kurland¹, Spencer Frome^{1,4}, Shrutika Singh¹, Jeff Zhang^{1,6,7}, Eunice Yang^{1,8}, Ki Yun Park^{2,3}, Cordelia Orillac¹, Aly A. Valliani¹, Sean Neifert¹, Albert Liu¹, Aneek Patel¹, Christopher Livia¹, Darryl Lau¹, Ilya Laufer¹, Peter A. Rozman¹, Eveline Teresa Hidalgo¹, Howard Riina^{1,9}, Rui Feng¹⁰, Todd Hollon¹¹, Yindalon Aphinyanaphongs^{6,7}, John G. Golfinos^{1,12}, Laura Snyder¹³, Eric Leuthardt², Douglas Kondziolka^{1,14}, Eric Karl Oermann^{1,9,15,16}

1. Department of Neurological Surgery, NYU Langone Health, New York, 10016, USA
2. Department of Neurosurgery, Washington University in Saint Louis, Saint Louis, MO 63110, USA
3. Washington University School of Medicine, Saint Louis, MO 63110, USA
4. New York University Grossman School of Medicine, New York, NY 10016, USA
5. Nomic AI, New York, NY 10003, USA
6. Department of Population Health, NYU Langone Health, New York, NY 10016, USA
7. Division of Applied AI Technologies, NYU Langone Health, New York, NY 10016, USA
8. Columbia University Vagelos College of Physicians and Surgeons, New York, NY, USA
9. Department of Radiology, NYU Langone Health, New York, NY 10016, USA
10. Department of Neurosurgery, Mount Sinai Health System, New York, NY 10019
11. Department of Neurosurgery, University of Michigan, Ann Arbor, MI 48109
12. Department of Otolaryngology - Head and Neck Surgery, NYU Langone Health, New York, NY 10016, USA
13. Department of Neurosurgery, Barrow Neurological Institute, Phoenix, AZ 85013, USA
14. Department of Radiation Oncology, NYU Langone Health, New York, NY 10016, USA
15. Center for Data Science, New York University, New York, NY 10011, USA
16. Neuroscience Institute, NYU Langone Health, New York, NY 10016, USA

Corresponding author during review

Anton Alyakin
 NYU Langone Department of Neurosurgery
 550 First Ave
 New York, NY 10016
Anton.Alyakin@nyulangone.org

Corresponding author post-review

Eric K. Oermann
 NYU Langone Department of Neurosurgery
 550 First Ave
 New York, NY 10016
Eric.Oermann@nyulangone.org

Abstract

Research in AI for Science often focuses on using modern AI technologies to augment components of the scientific process¹, or in some cases, the entire scientific method²; how about AI for scientific publications^{3,4}? Peer-reviewed journals are foundational repositories of specialized knowledge, written in discipline-specific language that differs significantly from general Internet content used to train most large language models (LLMs) and vision-language models (VLMs). We hypothesized that by combining a family of scientific journals with generative AI models, we could invent novel tools for scientific communication, education, and clinical care. We converted 23,000 articles from *Neurosurgery Publications*⁵ into a multimodal database - NeuroPubs - of 134 million words and 78,000 image-caption pairs to develop six datasets for building AI models. We showed that the content of NeuroPubs uniquely represents neurosurgery-specific clinical contexts compared with broader datasets and PubMed. For publishing, we employed generalist VLMs to automatically generate graphical abstracts from articles. Editorial board members rated 70% of these as ready for publication without further edits. For education, we generated 89,587 test questions in the style of the ABNS written board exam, which trainee and faculty neurosurgeons found indistinguishable from genuine examples 54% of the time. We used these questions alongside a curriculum learning process to track knowledge acquisition while training our 34 billion-parameter VLM (CNS-Obsidian). In a blinded, randomized controlled trial, we demonstrated the non-inferiority of CNS-Obsidian to GPT-4o ($p = 0.1154$) as a diagnostic copilot for a neurosurgical service. Our findings lay a novel foundation for AI with Science and establish a framework to elevate scientific communication using state-of-the-art generative artificial intelligence while maintaining rigorous quality standards.

1.1 Main

Scientific publications have existed in some form for millennia, stretching back to early works on medicine and mathematics from ancient Egypt⁶. While the nature of the medium has shifted over the years, the primary purpose has always been the communication and storage of knowledge within scientific disciplines in higher education and professions across society. Since the earliest modern journal publication by the Royal Society in 1665⁷, experiments in publishing have been driven by either the unique demands of the underlying fields or the emergence of novel media. In recent decades the dissemination of science has been impacted by the internet and rapidly-evolving media facilitated by it. Starting with the arXiv launch in 1991, preprints and whitepapers have become a common medium for sharing state-of-the-art scientific results for many fields in the physical, mathematical, and more recently - biomedical sciences (bioRxiv). Over the past few years, blog posts and graphical abstracts have emerged as novel means of communicating findings in a more widely available and digestible format, sometimes accompanied by peer-reviewed publications or preprint technical reports. The emergence of generative AI technologies in the form of large language models (LLMs)⁸ and vision-language models (VLMs)⁹ has raised new opportunities and challenges for scientific publishing⁴.

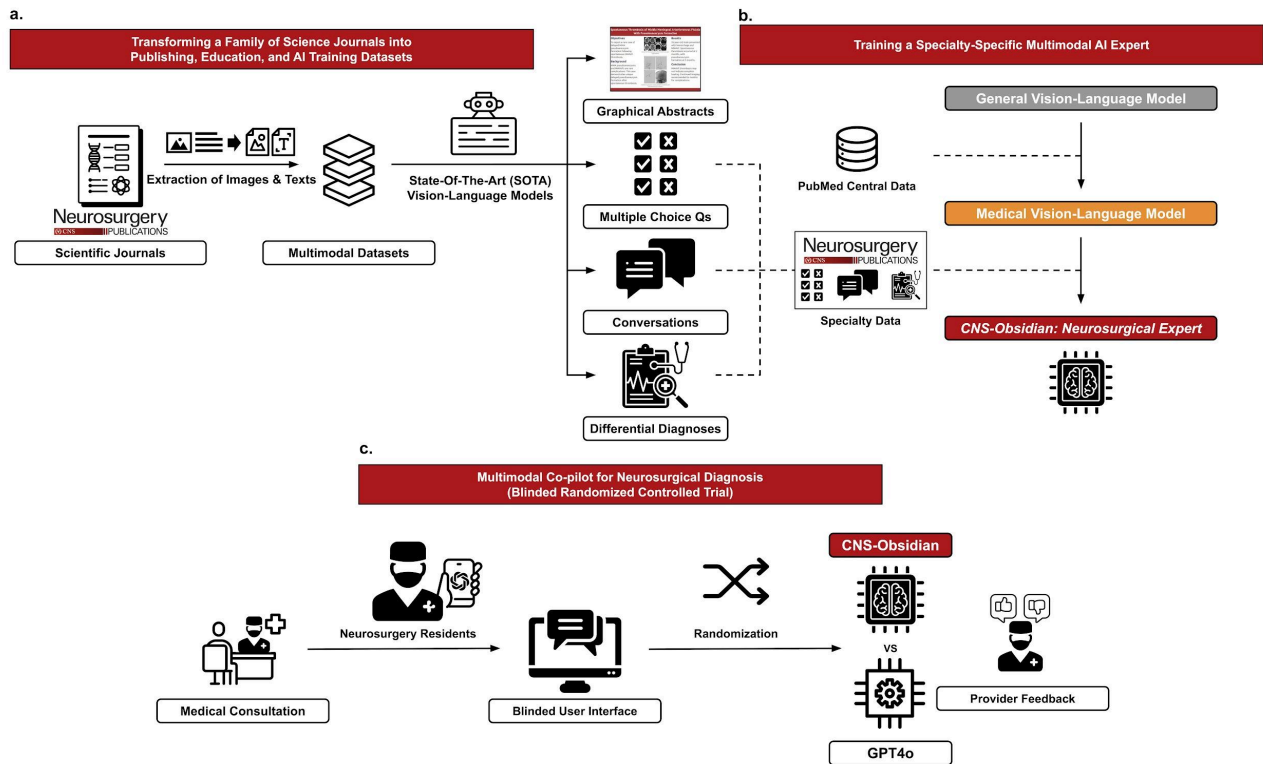


Fig. 1. Overview of our contributions. **a**, We developed a pipeline for the acquisition, extraction, and filtering of figures, captions, and in-text mentions from a family of biomedical journals. We also converted this data from unstructured biomedical texts and images into publishing, educational, and task-specific AI training datasets. **b**, We trained CNS-Obsidian, a 34B parameter autoregressive vision-language model that is domain-specific to neurosurgery with a novel training step designed to specifically entrain capabilities in differential diagnosis while maintaining ability to converse and answer questions. **c**, We ran a blinded, randomized controlled trial comparing CNS Obsidian to GPT-4o as diagnostic copilots on a busy inpatient surgical service.

One of the most critical components of generative AI models is their training data¹⁰, which in many cases is scraped from the Internet. Despite the size of the Internet, obtaining large, verified, and well-curated scientific datasets is difficult. This difficulty is compounded for multi-modal datasets (e.g., vision-language), or in low-resource domains such as many scientific and medical fields. Many attempts at using generative AI for Science^{1,11} have relied on datasets assembled with great effort and cost by the scientific community such as the Protein Data Bank¹² for AlphaFold¹, or the gnomAD¹³ dataset for AlphaMissense¹¹. Other efforts have focused on training LLMs and VLMs using the scientific literature itself by scraping PubMed abstracts¹⁴, PubMed Central articles¹⁵, or more diverse sources such as Twitter¹⁶.

However, all of these efforts are not able to access the meticulously curated, peer-reviewed, and highly specialized knowledge stored within limited-access journals on an article and sub-article level. It is possible that the highly curated content within families of scientific journals can, like the large datasets assembled by scientific communities, similarly lead to transformative generative AI applications of doing AI for Science by training AI with these scientific publications. We hypothesize that state-of-the-art vision-language models combined with an entire family of scientific journals could lead to novel tools that improve publishing, education, and practice (**Fig. 1a**).

1.1.1 Key contributions

Neurosurgery Publications is the journal of the *Congress of Neurological Surgeons* and a primary scholarly venue for the field of neurological surgery. It consists of three major journals, *Neurosurgery*, *Operative Neurosurgery*, and *Neurosurgery Practice*, and is published monthly by Wolters Kluwer under the current Editor in Chief, Dr. Douglas Kondziolka. We converted all three journals from *Neurosurgery Publications* into a large AI training dataset and performed an exploratory data analysis to compare the scientific content of our journal family to broader AI training datasets. Building from these datasets, we go on to make the following key contributions:

- (1) **Publishing**: We utilized a generalist VLM and our datasets to generate quick graphical abstracts for inclusion in *Neurosurgery Publications* (**Fig. 1b**).
- (2) **Education**: We generated tens of thousands of board review questions in the style of the American Board of Neurosurgery (ABNS) and subsequently utilized them for human and VLM training.
- (3) **Generative AI training**: We trained a specialty-specific VLM (CNS-Obsidian) using a novel curriculum learning pipeline with multiple choice question (MCQ) probes for a differential diagnosis task (**Fig. 1c**).
- (4) **Clinical care as a diagnostic co-pilot**: We deployed CNS-Obsidian with a chat interface as a point-of-care diagnostic co-pilot for neurological diagnoses and compared against a frontier VLM (GPT-4o) in a blinded randomized controlled trial (**Fig. 1d**).

1.2 Results

1.2.1 Scientific journals are a rich source of quality, domain-specific data

We identified *Neurosurgery Publications* as a potential source of high quality scientific text and image data due to the rigorous peer-review and publishing processes. We used a variety of acquisition, extraction, and filtering tools to assemble a dataset of texts and images by retrieving and processing all of the available *Neurosurgery Publications* articles. A total of 23,984 articles were converted into a base dataset consisting of 139 million words and 78,853 scientific figures with captions. We called the resulting base multimodal dataset *NeuroPubs*, and utilized it for subsequently exploratory data analysis and AI training dataset construction.

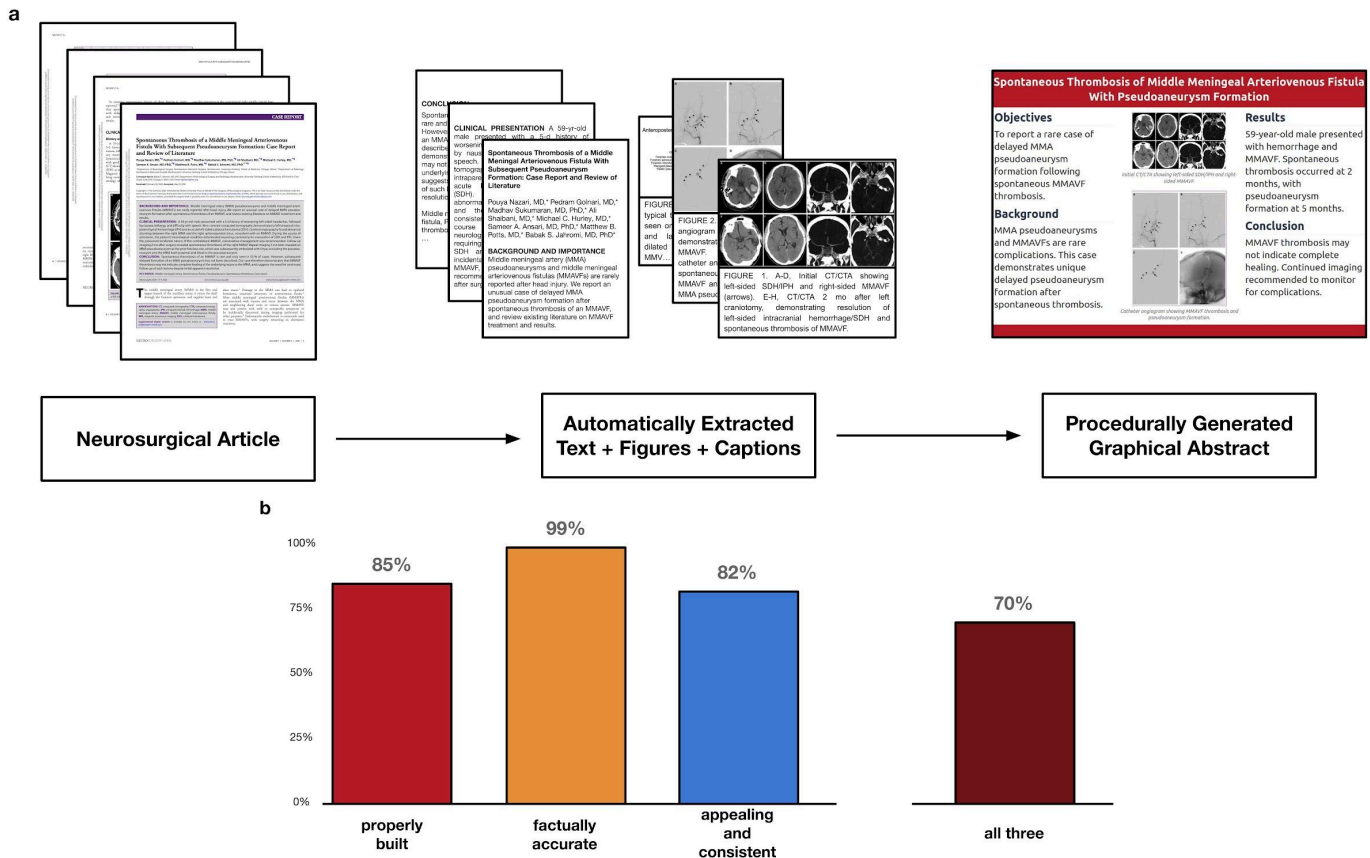


Fig 2. NeuroPubs and code-VLMs instantly create graphical abstracts

In order to investigate the use of NeuroPubs for disseminating scientific knowledge, we investigated the combination of NeuroPubs with Claude Sonnet-3.5 to rapidly generate graphical abstracts or presentation slides. **a**, A pipeline of converting full text articles to graphical abstracts. Text and figures sourced from *P. Nazari et al.*, Spontaneous Thrombosis of a Middle Meningeal Arteriovenous Fistula With Subsequent Pseudoaneurysm Formation: Case Report and Review of Literature. Graphical abstract simplified for visibility in the figure. **b**, Quality analysis of a 100 automatically generated abstracts by the members of the *Neurosurgery* Editorial Board. Articles were evaluated for 1) being properly built (true for 85% of abstracts), 2) being factually accurate (99%), 3) being visually appealing and consistent with journal expectations (82%). Also included is the proportion of articles that achieved all three criteria (70%).

1.2.2 Vision-language models create production-ready graphical abstracts

Neurosurgery Publications encourages the creation of graphical abstracts to accompany published articles. We developed a pipeline for the automatic conversion of articles in *NeuroPubs* into graphical

abstracts using CSS templates and iterative prompting of a frontier, generalist VLM (see Methods for details) (**Fig. 2; Extended Data Fig. 1**). One hundred automatically generated graphical abstracts were evaluated by *Neurosurgery Publications* Editorial Review Board members. Generated graphical abstracts were free of formatting errors 85% of the time, 99% of abstracts were factually correct, and 82% were found to be visually appealing. Graphical abstracts that were judged as being “publication ready” had to meet all three criteria, and 70% of the generated abstracts passed this bar without any manual involvement in abstract creation.

1.2.3 Converting a specialty journal into a multimodal AI dataset

The base *NeuroPubs* dataset was converted into three task-specific datasets for VLM visual instruction fine tuning (IFT) (n=127,076 samples, 4.2M tokens), multiple-choice questions (MCQs) (n=89,587, 3.7M tokens) for human and VLM assessment, and cases with differential diagnoses (n=46,401, 0.4M tokens) for training a diagnostic co-pilot (**Extended Data Fig. 2-3**). We explored the content of *NeuroPubs* relative to the broader PubMed dataset to assess how much unique content was contained in our journal relative to the broader medical literature - noting that this divergence would likely be greater for broader, internet-scale datasets. We found a marked divergence between these datasets (**Fig. 3a-c**).

1.2.4 NeuroPubs and generalist LLMs can make multiple choice questions for assessing medical trainees and VLMs

We assessed whether generalist VLMs, GPT-4o and Claude Sonnet-3.5, and *NeuroPubs* could be used to generate board examination questions for instructing both medical trainees and guiding VLM development. We generated 89,587 synthetic MCQ questions using frontier VLMs (see Methods). To assess generated sample quality, we randomly sampled 50 synthetic questions generated by two different frontier models and 50 real questions from the *Congress of Neurological Surgeons (CNS) Self-Assessment of Neurological Surgery (SANS)* and used these to generate multiple 30 question mock exam blocks which randomly contained real and synthetic questions. We found that the average quality of questions made in a fully automated way is not yet at the level of manually created and curated ones with an average of 25% of the AI generated questions being rated as good board review questions compared to 72% of the Human generated questions ($p < 10^{-7}$) (**Extended Data Fig. 4**). 54% of AI-generated questions misled at least one evaluator into thinking that they were Human-made, and 23% misled both.

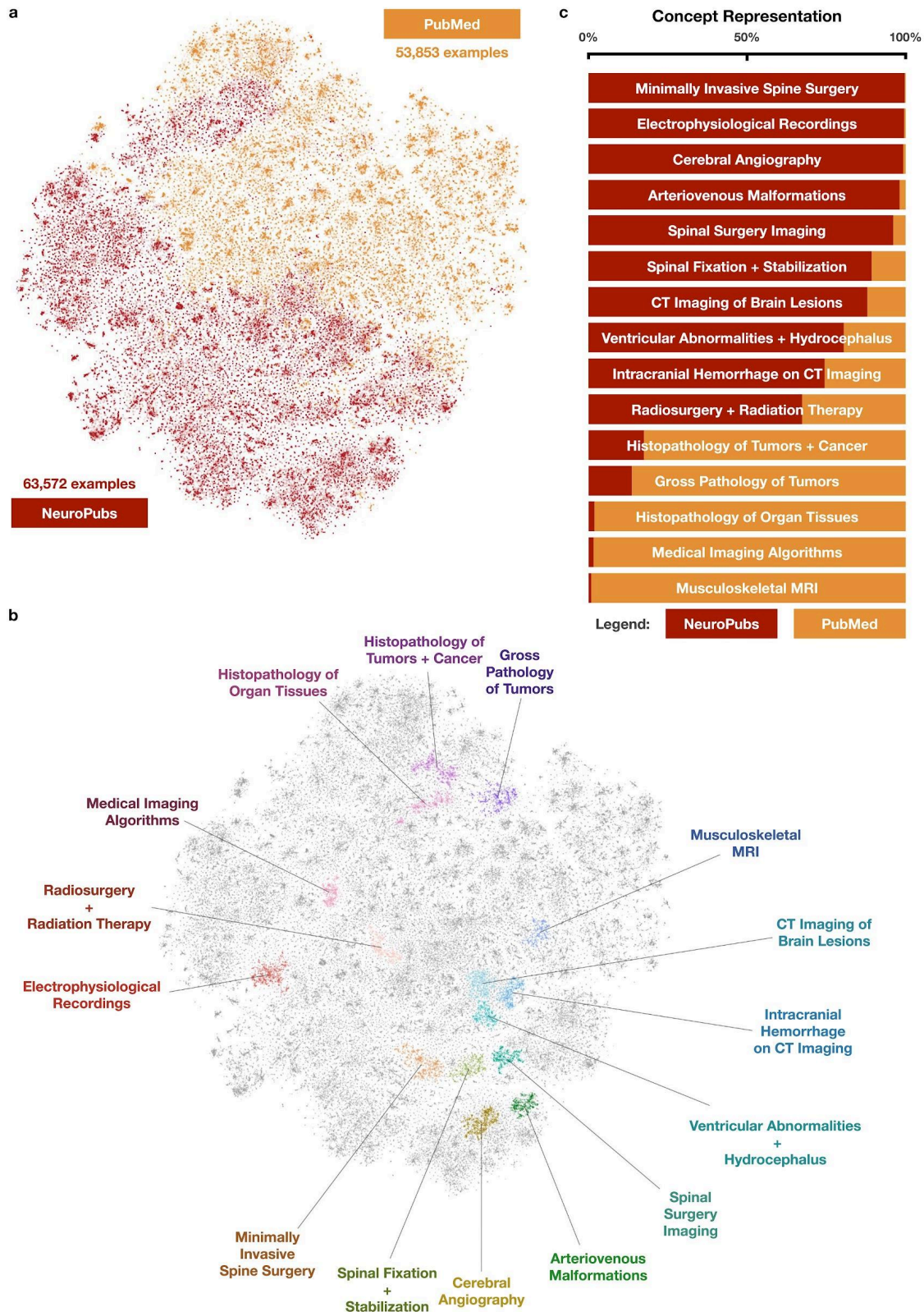


Fig. 3. The NeuroPubs dataset. **a**, A joint embedding of the PubMed-based and Neurosurgery-based instruction fine-tuning datasets. There is a notable lack of overlap between content contained within NeuroPubs and the broader medical dataset within PubMed. **b**, The 15 largest topics in the data. **c**, Comparison of the percent composition of 15 largest clusters in the datasets. NeuroPubs is particularly dense in the highly-specialized neurosurgical topics.

1.2.5 Building multimodal neurosurgical artificial intelligence

We trained a specialty-specific VLM using NeuroPubs and a fully-autoregressive VLM architecture¹⁷(**Extended Data Fig. 5a**). We extended the generalist medical curriculum training¹⁵ by introducing a third stage designed to learn specialty-specific knowledge through instruction finetuning, the skill of differential diagnosis, and answering specialty-specific multiple-choice questions (**Fig 4a-b; Extended Data Fig. 5b**). We performed extensive ablations and experiments, and used our MCQ performance as a means of quantitatively evaluating model knowledge acquisition during Stage 3 training as a probe for differential diagnosis abilities (**Extended Data Fig. 6-8; also see Supplemental Methods: Ablations**). Our best performing model matched GPT-4o's performance on the held-out GPT-generated MCQs ($p = 0.2347$) (**Fig. 5c**) and substantially outperformed both GPT-4o and Claude Sonnet-3.5 on the Claude-generated MCQs ($p = 0.0011$ and 0.0004 , respectively), despite being exclusively trained on the GPT-generated data (**Fig. 5d**). Zero-shot performance on the human-generated CNS-SANS questions improved from a baseline of 39.81% to 46.81%, but was unable to match the state-of-the-art frontier models (GPT-4o = 65.70%, $p < 10^{-15}$) (**Fig. 5e**) which we hypothesized was likely due to data contamination within the frontier models. Including additional Claude-generated data in the model training improved the performance on Claude generated MCQs ($p = 0.0427$) but did not on GPT generated MCQs ($p = 1.000$) or SANS ($p = 0.5193$).

1.2.6 Specialty-specific VLMs are effective diagnostic co-pilots at the point of care

We developed a platform for deploying VLMs internally within our health system. Using this platform we implemented a chatbot interface for our VLM (**Extended Data Fig. 9**). We launched a blinded, randomized controlled trial of our specialty VLM, CNS-Obsidian, vs. GPT-4o as point-of-care diagnostic co-pilots for three months of deployment (**See Supplemental Information: Trial Protocol**). For three months, neurosurgical residents at a major academic medical center were provided with a web-app that provided a chat interface for interacting with a VLM. The VLM was conditioned to provide a differential diagnosis based on user-provided visual and text inputs and the backend model was randomized between GPT-4o and CNS-Obsidian (**Fig. 5a; Extended Data Fig.10, Supplementary Video 1 and 2**). For our primary endpoint of noninferiority for a clinically helpful differential diagnosis CNS-Obsidian was found to have an upvote frequency of 40.62%, non-significantly lower than the GPT's 57.89%. ($p = 0.1150$) (**Fig. 5b**). For our secondary endpoint of follow-up conversation diagnostic helpfulness, CNS-Obsidian was also found to have non-significantly lower upvote frequency at 25.00% vs. 40.00% of GPT-4o ($p = 0.1266$) (**Fig. 5c**). Both models were assessed on the correctness of the generated differential diagnoses, measured as including the final diagnosis in the generated list at the time of the consult. Here, CNS-Obsidian achieved a score of 59.38% compared to GPT-4o's of 65.79% ($p = 0.3797$) (**Fig. 5d**). Noting that GPT-4o tended towards broader and lengthier differentials (**Fig. 5a**), we corrected for length and found that CNS-Obsidian trended towards a higher rate of correct diagnoses 16.88%, compared to GPT-4o's of 10.69% ($p = 0.9590$) (**Fig. 5e**). For our other secondary endpoint of user engagement, assessed as the length of the continued conversation, CNS-Obsidian had an average conversation length of 2.50 compared to GPT-4o's of 1.79 ($p = 0.6719$) (**Fig 5f**). Notably, there were a total of 70 chats (average of 0.75 per day; 38 randomized to GPT-4o, 32 randomized to CNS-Obsidian) over the data collection period of 92 days. During this time period, 959 consults overall (10.42 per day) were seen by the Neurosurgery service.

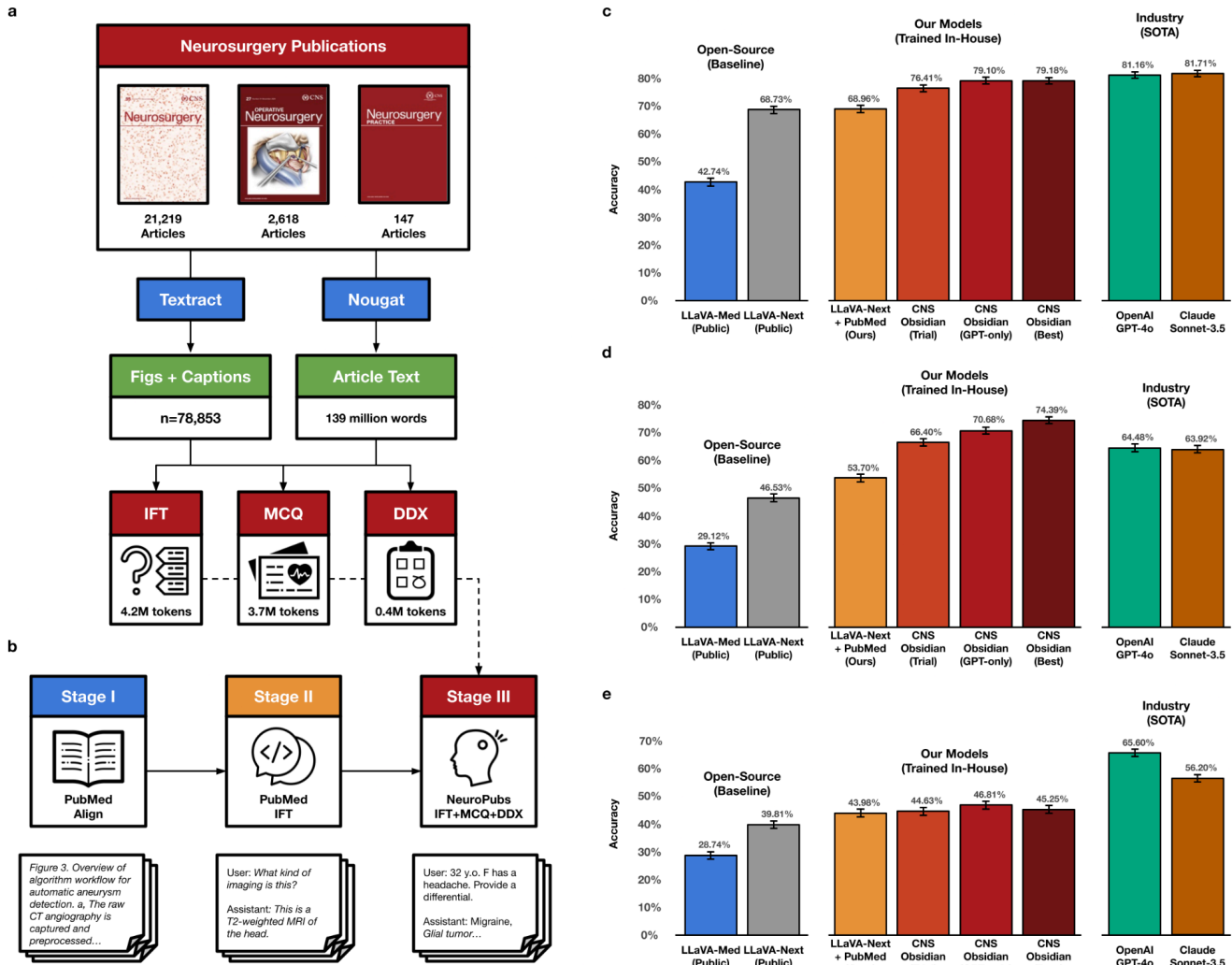


Fig.4. Dataset, curriculum training, and benchmark performance. **a**, Acquisition, processing, and knowledge translation pipeline for converting our specialty journal into an AI knowledge database (139 million words, 78,853 captioned figures) and subsequently into task-specific vision-language datasets. **b**, Our approach includes a novel stage in training a medical VLM that is specific to a specialty, neurosurgery, and to a downstream task, diagnosis, while preserving the general conversation and question-answering capabilities. **c**, Best CNS-Obsidian model trained on only GPT-data statistically matches GPT-4o on the held-out GPT generated MCQs questions ($p = 0.2161$). There is no difference between best CNS-Obsidian trained on GPT only and one trained on both datasets ($p = 1.000$) **d**, Best GPT-Synthetic trained CNS-Obsidian model configuration outperforms both GPT-4o ($p = 0.0011$) and Claude Sonnet 3.5 ($p = 0.0004$) on Claude generated MCQs synthetic questions. The performance improves when retrained on a mix of both GPT-Synthetic and Claude-Synthetic data ($p = 0.0427$). **e**, CNS-Obsidian improves over the baseline on the one-shot neurosurgery board-like questions, but remains inferior to the state-of-art-models ($p < 10^{-15}$ versus GPT-4o). Performance does not change significantly after retraining with Claude-generated data included ($p = 0.5193$).

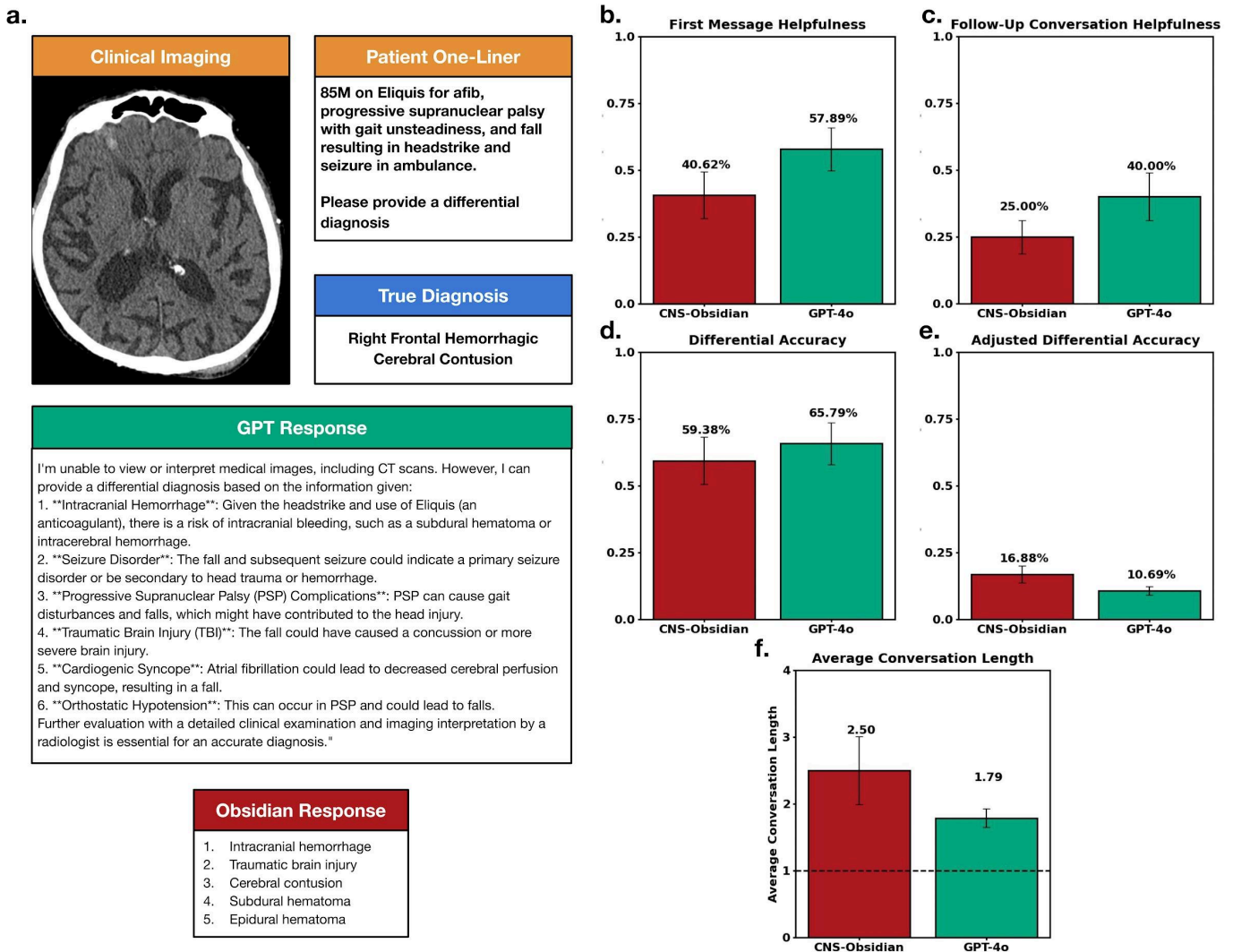


Fig. 5. Randomized controlled trial results. **a**, Example patient encounter (identifying details anonymized) submitted by a resident to the trial interface. The patient was randomized to the GPT arm. Outputs from GPT, counterfactual CNS-Obsidian output, and the true diagnosis are shown. GPT generated broader but less specific differentials with a conversational tone. **b**, Primary Endpoint: Diagnostic helpfulness (user-rated). CNS-Obsidian was found to be non-inferior to GPT-4o in the frequency of upvotes on the first message. ($p = 0.1150$). **c**, Secondary Endpoint: Clinical helpfulness of follow-up chats (user-rated). CNS-Obsidian was found to be non-inferior to GPT-4o in the frequency of upvotes on the first message. ($p = 0.1266$). **d**, Secondary Endpoint: Diagnostic accuracy, measured by inclusion of the true diagnosis in output lists. CNS-Obsidian differentials included the correct diagnosis ($p = 0.3797$). **e**, Adjusted Secondary Endpoint: Average proportion of accurate diagnoses within differentials. CNS-Obsidian suggested diagnosis is more likely to be correct on average, indicating non-inferiority ($p = 0.9590$). **f**, Secondary Endpoint: Average conversation turn length (baseline = 1.0). Conversations randomized to CNS-Obsidian tended to be non-significantly longer ($p = 0.6655$).

1.3 Discussion

We present our attempt to repurpose scientific and medical journals using VLMs in an era of generative AI - doing AI for Science by building *AI with Science*. By integrating *Neurosurgery Publications* with VLMs for publishing, education, AI modelling, and clinical care we show how

repurposing quality scientific content can push the boundaries of generative AI, and create a mutually beneficial relationship between VLMs and the scientific literature. VLMs can augment scientific publications by rapidly generating novel and accurate educational and publishing content. In turn, scientific publications can augment VLMs with curated, multimodal data. By defining scientific journals as knowledge resources for human *and* AI training, we envision an exciting future for scientific publishing through the intelligent use of these tools.

We converted *Neurosurgery Publications*, the medical journal family of the *Congress of Neurological Surgeons*, into an AI training dataset and used that dataset to build a 34B parameter VLM using state-of-the-art techniques and a novel training regimen to emphasize differential diagnostic reasoning. To ensure a rigorous comparison on all downstream tasks, we held out entire articles from the training datasets to ensure that CNS-Obsidian never saw the underlying content at any step in its training. Due to unknowns surrounding the underlying training datasets of GPT-4o and Claude Sonnet-3.5 and known instances of data leakage^{18,19}, we believe this to be an exceptionally strict control for potential data contamination. We found that CNS-Obsidian performed comparably to the state-of-the-art frontier models, OpenAI's GPT-4o and Anthropic's Claude Sonnet-3.5, on real and synthetic domain specific (neurosurgery) multiple choice questions. These results emphasize the importance of in-domain data and that *data is the most important aspect of modern AI efforts* which overwhelmingly benefit from the massive availability of information on the internet. Where high quality medical information is typically *not* publicly available on the internet scientific publications present an immediate solution. Part of what makes publications so valuable is the multimodal paired image-text information, which is particularly rare. While efforts exist to directly scrape this content from Twitter¹⁶, or to utilize publicly available resources¹⁵, these efforts are likely noisier than scientific images with expertly authored captions such as those found in refereed journals.

As part of this project we conducted the first blinded, randomized controlled trial of VLM chatbots in a clinical setting. Unlike prior works that used randomization and blinding in simulated clinical settings^{20,21}, our trial captured the complexities of real-world care. Both CNS-Obsidian and GPT-4o were seen as helpful at the point of care almost half of the time, and rated similarly on engagement despite GPT-4o's longer and more verbose messages. While both models included the correct diagnosis in their differentials over half the time, CNS-Obsidian produced more precise differentials compared to GPT-4o's broader and less specific differentials. While prior works on enabling LLMs for differential diagnostic reasoning utilized large, close source LLMs with prompting schemes²⁰, we directly finetuned our model on vision-language cases with paired differential diagnoses sampled from journal content, tailoring it more closely to the clinical environment.

One of the most significant findings of our RCT was the low utilization of the chatbot by neurosurgical participants. We attribute this low utilization rate due to the chatbot user interface itself - highly trained specialists would prefer automated solutions that free up their time to accomplish tasks rather than assistance with completing the tasks themselves. We hypothesize that one major barrier could be the chatbot interface itself, and the need to spend more time taking photos and texting responses which, for specialists, is largely unnecessary which might not hold true for generalist users. Notably, despite the differential diagnoses frequently being perceived as helpful, both cases frequently *did not contain the final, official diagnosis*.

1.4 Limitations

We acknowledge several key limitations in our work to “repurposing scientific publications”. We performed an exhaustive set of ablations to help identify the most beneficial training recipe and data mixture for our VLM configuration. However, we restricted ourselves to fully autoregressive models and did not explore cross attention-based alternatives²². Other potential model improvements, such as grounding strategies to more closely align fine-grained text and image features, are left to future researchers investigating medical VLM architectures. We also note that we restricted ourselves to utilizing *only* the content from a single journal family, *Neurosurgery Publications*, rather than the entirety of the neurosurgical literature. Comparisons against frontier models also were limited by our ability to evaluate for data leakage due to the lack of transparency surrounding the training datasets of these models. Our blinded RCT was limited by a low response rate, resulting in a relatively small sample size, and by its conduction at a single institution. These factors may limit the generalizability of our findings and underscore the need for future multi-center studies with larger numbers of participants. The low response rate itself is an interesting finding and raises several hypotheses as to ways of improving human-AI interactions in the medical setting, echoed by a recent study in Greece where surgeons had more negative perceptions of a GPT-4 based chatbot than their medical counterparts²³. One is by eliminating the need for conversational (chatbot) user-interfaces, as busy physicians may prefer to not use tools requiring substantial user-inputs in order to get a response. A second is that non-specialists may ultimately be more receptive audiences, where their broader scope of practice may see greater benefits from interacting with a chatbot’s stored knowledge.

A further limitation is our design choice to do full pre-training and finetuning of CNS-Obsidian, as compared to prompting and zero-shot inference with GPT-4o. Furthermore, it may be possible that with additional techniques such as retrieval augmented generation (RAG)²⁴, or additional uses of in-context learning or CoT prompting that both models could have improved performance as has been demonstrated in other works²⁵. These observations highlight the need for more research into human-AI interactions in real-world environments as well as alternative user interfaces beyond chatbots to better align with specialist workflows.

1.5 Conclusion

We present here our results of doing *AI with Science*, and combining state of the art VLMs with a scientific journal family. Reinventing a scientific journal family, *Neurosurgery Publications*, with VLMs ultimately lead to potential benefits for both the journal and its scientific field. Automating the generation of graphical abstracts can expedite the communication of information, while the generation of board review questions can help with assessing educational achievement and minimizing the workloads of faculty members. Directly training journal content into the weights of a thirty-four billion parameter VLM lead to competitive results on specialty MCQ assessments with frontier models and in a real-world clinical deployment as a diagnostic co-pilot as compared to GPT-4o, a closed-source VLM rumored to be in the trillions of parameters and widely acknowledged as the generalist state-of-the-art. These results suggest a possible role for mesoscale VLMs built by scientific and medical communities using unique community data resources to address unique community needs. While this project focuses on neurological surgery, it is easy to imagine alternative works for other areas of science and medicine.

Methods

2.1 IRB and Legal

This project was approved by the NYU Langone Institutional Review Board (i23-00510). This project was also reviewed by the leadership of *Neurosurgery Publications* and Wolters Kluwer. All parties agreed to the utilization of journal content for the purposes of this study. *Self-Assessment of Neurological Surgery* questions were utilized as a benchmark with the permission from the *Congress of Neurological Surgeons*.

2.2. Data Acquisition and Processing

We built a pipeline to create a dataset from three neurosurgical journals: *Neurosurgery* n=21,219, *Operative Neurosurgery* n=2,618, *Neurosurgery Practice* n=147. We implemented two parallel extraction streams. For images, AWS Textract identified figure locations and generated bounding boxes for cropping. Our regex-based caption matcher paired images with candidate captions using geometric distances. For text, we used a combination of AWS Textract and Meta's Nougat²⁶ to extract unstructured texts from the PDFs. We used regular expressions to identify in-text mentions of each figure within the texts and stored these excerpts together with the figure's caption and metadata.

2.3. Graphical Abstract Generation

2.3.1 Generation Pipeline

We developed an automated pipeline to convert extracted manuscript content into standardized graphical abstracts. The pipeline implements a custom Cascading Style Sheet (CSS) profile designed to match the format of existing Neurosurgery graphical abstracts. Using Claude Sonnet-3.5, we engineered prompts to generate structured HTML summaries compatible with our CSS profile. The summaries were organized into six sections: Objectives, Background, Methods, Results, Discussion, and Conclusion. The model also selected up to two representative figures from each manuscript based on caption analysis.

2.3.2 Abstract Human Evaluation

We evaluated the pipeline's performance using a random sample of 100 articles published between 2021-2024. Three members of the Neurosurgery Editorial Review Board assessed each generated abstract using three binary criteria:

- Graphical Abstract is Properly Built? (0: No, 1: Yes)
- Content is Factually Correct? (0: No, 1: Yes)
- Graphical Abstract "Looks Good" for our Journal? [Good figure choice? Good facts to include?] (0: No, 1: Yes)

2.4 Knowledge Translation Framework

2.4.1 Filtering

We built an image content classification system using ResNet-50²⁷ feature extraction followed by a linear classifier. In order to do so, we manually annotated 500 figures as one of three classes:

- Class 2: Medical imaging (CT, MRI, X-ray, angiography)
- Class 1: Clinical visuals (surgical fields, microscopy, anatomical drawings)
- Class 0: Technical content (flowcharts, survival curves, tables)

We extracted last layer ResNet features from 400 of these images, trained a linear classifier on them, and validated its performance on the remaining 100 (**Extended Data Fig. 1**). We then applied the filtering to the remainder of our dataset. We did so twice, once learning to differentiate Class 2 from the other two, for the purpose of identifying differential diagnosis dataset candidates, and once to differentiate Classes 2 and 1 from the technical consent, for the purpose of identifying images that can be converted into interesting multiple choice questions. Candidates for the instruction fine-tuning dataset included all three classes. All conversion candidates underwent basic filtering requiring >100 characters of combined caption and in-text mentions.

2.4.2 Conversion

We developed an automated pipeline using OpenAI GPT-4o and Anthropic Claude Sonnet-3.5 to convert specialized domain knowledge into high-quality training data for vision-language models:

1. Instruction fine-tuning (IFT): Conversational pairs
2. Multiple-choice (MC): Clinical vignettes with options
3. Differential diagnosis (DDx): One-line case summaries with ranked diagnoses

Each generation task used custom prompts with four randomly sampled few-shot examples from a pool of 10 examples (IFT used LLaVA-Med¹⁵ examples; MC and DDx were manually created by us). Models were prompted to create a user-assistant conversation, a multiple choice question with discussion, or a patient one liner with a differential diagnosis based on the image, caption, and in-text mention, but without explicit reference to the latter two. The pipeline included the target figure in the API call but excluded example figures.

2.5. Dataset Visualization

2.5.1 Data Cartography

We embedded the text portion of the IFT dataset obtained from passing *Neurosurgery Publications* through GPT, together with a dataset generated in the same methodology from *PubMed*¹⁵, into a shared two-dimensional space for visualization and data exploration purposes. To do so, we first used Nomic Embed Text v1²⁸, an open-source BERT-like text embedder that converts unstructured text into 512-dimensional vectors. We subsequently used tSNE²⁹ to reduce the dimensionality to two dimensions. We obtained 12 largest clusters using the HBDSCAN³⁰ hierarchical clustering and generated names for it by sampling texts from inside and outside the cluster and making a query to GPT-4o asking to come up with a name that unifies the themes of the cluster.

2.6 Multiple Choice Evaluation

2.6.1 MC Human Evaluation

We developed five surveys, each consisting of 10 authentic questions from the neurosurgical boards question bank (*Self-Assessment for Neurological Surgeons*, SANS) and 20 synthetic questions—10 generated by GPT-4o and 10 by Claude Sonnet 3.5—presented in a blinded and randomized order. To maintain consistency with our image-based synthetic datasets, only image-associated questions from the SANS question bank were included. Synthetic questions were sourced exclusively from holdout datasets to ensure none were present during model training. Each survey was administered to one neurosurgery trainee (resident) and one attending neurosurgeon. For each question, participants answered two follow-up questions: (1) whether they believed the question was human- or

AI-generated, and (2) whether the question was suitable for neurosurgery board preparation. In addition to human evaluations, we assessed question-answering performance using the state-of-the-art vision-language model GPT-4o. Subsequently, we tested our best specialist model, CNS-Obsidian-final-both ([5, 10, 10]-both), on the same dataset. Two-sided Fisher's exact tests were performed on the outcomes of interest - human-evaluated question source and question quality.

2.7. Model Architecture and Training

2.7.1 Vision-Language Model Backbone

LLaVA (Large Language and Vision Assistant) combines vision and language processing by aligning CLIP-derived image features with language embeddings, enabling interactive image understanding. We built on LLaVA-Next's improvements - including its multilayer projection, patch-based processing of large images, and enhanced pre-training. (**Extended Data Fig. 4a**) As a starting point, we used the 34B parameter version of LLaVA-Next based on Nous Hermes 2 Yi-34B available on HuggingFace Transformers.

2.7.2 Three-Stage Curriculum Training

We developed a training protocol based on the LLaVA-Med curriculum training, but with a novel Specialization Stage 3. Stage 1 ("alignment") kept the model frozen while training only projection layers on PubMed-based figure-caption pairs. Stage 2 ("medical knowledge integration") unfroze both projection and language model components and train on general medicine PubMed-based conversations (IFT) dataset generated using GPT-4o. Stage 3 ("neurosurgical specialization") maintained the same unfrozen components while training on our domain-specific, *Neurosurgery Publications*-based, and task-specific (IFT, MC, and DDx) datasets generated using GPT-4o and Claude Sonnet 3.5. (**Extended Data Fig. 4b**)

2.7.3 Training Details

The training infrastructure used 104 H100s on NYU Langone's UltraViolet high-performance compute cluster. PyTorch FSDP was used for distributed data parallelization. We used bfloat16 precision, with learning rates of 1e-3 for Stage 1 and 1e-5 for Stages 2 and 3, and cosine scheduling. Mini-batch size per GPU was 4, with gradient accumulation steps of 4 during Stage 1, yielding effective batch sizes of 1664 for Stage 1 and 416 for Stages 2 and 3 across our distributed setup. Unlike LLaVA-Next, but similar to LLaVA-Med, we kept the vision encoder frozen due to training stability constraints. Data splits maintained paper-level separation with 95% training, 2.5% validation, and 2.5% test sets to prevent information leakage between splits. Validation was used to monitor loss, whereas test split was used to establish performance (see Methods 2.8.2).

2.7.4 Training Length

We refer to different checkpoints of our model as [*<# of Stage 1 epochs>*, *<# of Stage 2 epochs>*, *<# of Stage 3 epochs>*] for brevity and convenience. We started with recreating LLaVA-Med's framework, but using LLaVA-Next architecture, with one epoch of Stage 1 training and three epochs of Stage 2 training, yielding our LLaVA-Next-Med [1, 3, 0]. In the initial attempt of creating a task-specific model, we trained this model on three epochs of GPT-Only Stage 3 datasets, yielding [1, 3, 3]. Through extensive experiments and ablation studies (See Supplemental Results: Ablations) we found that the standard training duration of 1 epoch for alignment and 3 epochs for medical and neurosurgical fine-tuning was insufficient for a model of this scale (**Extended Data Fig. 5-6**). Our best performing

model ended up being extensively trained [5, 10, 10]. Throughout our training length experiments we only used GPT-sourced data for training. We also experimented with training this model on Claude and GPT-based data together, trying both the constraint for epoch number and compute amount (**Extended Data Fig. 7**). Wall-clock training time per epoch was 3.5 hours for Stage 1, 30 minutes for Stage 2, and 1 hour for Stage 3 using only one data source (e.g. only GPT-4o) and 2 hours if using both GPT-4o- and Sonnet 3.5-based datasets.

2.8 Evaluation

2.8.1 Benchmarking

We evaluated LLaVA-Next-Med and CNS-Obsidian against multiple baselines: LLaVA-Med, base LLaVA-Next, OpenAI GPT-4o, and Anthropic Claude Sonnet 3.5. For our models, LLaVA-Med, as well as LLaVA-Next we used vLLM for deployment and made calls to the deployed model via requests interface. For GPT-4o and Sonnet 3.5 evaluations, we made direct API calls to the publicly available checkpoints. We used a local instance of LLaMA-70B to parse the models' chain-of-thoughts and convert them to single-letter answers for automated matching against ground truth. We used two-sided Fisher exact tests to establish significance or a lack of there-off throughout benchmarking.

2.8.2 Synthetic Domain-Specific Questions

We created additional synthetic benchmarks from our held-out test data (2.5% of total), comprising 1,282 questions from the GPT-Synthetic dataset and 1,239 questions from the Claude-Synthetic dataset. Paper-level splitting during training ensured these test questions contained neither previously seen questions nor figures from training papers. We used these benchmarks to guide our decisions with ablations.

2.8.3 Human-Made Domain-Specific Questions

The *Self-Assessment of Neurological Surgery* (SANS) questions formed our primary benchmark. These questions, designed by the Congress of Neurological Surgeons (CNS), are used by neurosurgery residents preparing for American Board of Neurological Surgeons standardized examinations. The CNS provided 3,965 questions for our evaluation set. Of these questions, 950 contained question-associated images, which formed our benchmark.

2.9 Randomized Control Trial

2.9.1 Interface and Evaluation Stack

Our final evaluation component involved a randomized controlled trial (RCT) comparing the diagnostic and consultation performance of NYU-Obsidian to a PHI-safe version of GPT-4o. To facilitate this, we developed a full-stack application for blinded and randomized evaluation of clinician-facing LLMs. The user interface (**Extended Data Fig. 8**) was adapted from a publicly available framework Chatbot UI, implemented in React and Next.js, and extended with features such as secure authentication, medical reference number recording, image submission, and endpoint randomization for each new session. The system utilized Postgres for account and chat storage, Flask with SQLiteDB for authentication, vLLM for hosting the local model (CNS-Obsidian), and Kong as an API gateway to connect with the PHI-safe OpenAI GPT-4o. Throughout the trial, the best-performing model at the beginning of the trial, CNS-Obsidian-base [1, 3, 3], was used, despite later improvements in training schema resulting in superior, longer-trained versions.

2.9.2 Randomization and Sample Size

Study participants included neurosurgery residents, fellows, attending physicians, and advanced practice providers, who interacted with a randomly assigned model in each conversation. The data was collected for three months, August 30th, 2024 through November 30th, 2024 on the Neurosurgery service at NYU Langone Health Tisch Hospital. All trainees and faculty in the department were invited to participate via email. They were instructed to interact with the software *after* finishing an encounter with a consult patient. Each chat was randomized independently of others using python's scipy binomial pseudorandomness.

The trial was not preregistered due to its observational nature as it's a user study of tools that were used after patient assessment, not before. The tools were not accessible during patient assessment. (See **Supplemental Information: User Manual** and **Supplemental Information: Trial Protocol**)

2.9.3 Diagnostic Helpfulness

Clinicians submitted medical images alongside concise clinical summaries ("one-liners"). Models were prompted to generate a differential diagnosis in their first response, which clinicians then rated as either clinically helpful ("thumbs up") or not ("thumbs down"). Clinicians could optionally continue the conversation, rating subsequent responses as well. The primary endpoint of the study was the subjectively rated diagnostic helpfulness of the first response, defined as the frequency of "thumbs up". Secondary endpoints included the length of follow-up conversations and the subjective helpfulness of these interactions, as well as post-hoc differential accuracy.

2.9.4 Differential Accuracy

For each submitted case, patient identifiers were recorded but omitted from model inputs. Ground truth diagnoses were retrospectively retrieved and compared against model-generated differential diagnoses. Accuracy of the differential diagnosis, measured as the proportion of cases where the true diagnosis appeared in the list of differentials served as an additional secondary endpoint. Evaluation involved a two-step automated process:

1. GPT-4o extracted individual diagnoses from the unstructured model outputs into a structured list.
2. GPT-4o determined whether the true diagnosis was included in this list.

During analysis, GPT-4o's differentials were observed to be longer and less specific compared to CNS-Obsidian. To address this, we introduced an adjusted accuracy metric: the average proportion of correct diagnoses divided by the differential list's length.

2.9.5 Statistical Analysis

The RCT was designed as a non-inferiority study using one-sided statistical tests:

- Diagnostic Helpfulness (both primary and secondary): Fisher's exact test, testing the hypothesis that CNS-Obsidian is less helpful than GPT-4o.
- Diagnostic Accuracy: Fisher's exact test, testing the hypothesis that CNS-Obsidian is less accurate than GPT-4o.
- Length-Adjusted Accuracy: Mann-Whitney U test, comparing fractions of correct responses adjusted for differential list length.

- Engagement Frequency: Mann-Whitney U test, comparing the frequency of clinician interactions to the number of submitted consults, testing the hypothesis that CNS-Obsidian is less engaging (has shorter chats).

End notes

3.1 Data availability

Data used for the general medicine stages of model training was downloaded using LLaVA-Med GitHub repository (<https://github.com/microsoft/LLaVA-Med>) and is publicly available. Data extracted from the *Neurosurgery Publications* was used with the permission of their leadership, but will not be made publicly available in either the raw (texts and images) or the converted (MCQ, IFT, DDx AI datasets) in any form as it is protected by respective copyrights and trademarks. We forward readers interested using this data to the *Neurosurgery Publications* as well as Wolters Kluwer. *Self-Assessment of Neurological Surgery (SANS)* questions used as a benchmark were used with permission of the *Congress of Neurological Surgeons (CNS)* and will not be made publicly available as they are intellectual property of the *CNS*. The clinical data was collected under the NYU Langone Institutional Review Board (i23-00510) and is protected by the Health Insurance Portability Accountability Act and other patient health information laws and will not be made publicly available, except for the anonymized example included in the figures. Icons were sourced from the Noun Project (<https://thenounproject.com/>).

3.2 Code availability

We used Python 3.10, 3.11, and 3.12, as well as many open-source libraries, including datamapplot 0.4.2, HuggingFace Transformers 4.44.0, matplotlib 3.9.1, numpy 1.26.4, openai 1.55.3, pandas 2.2.0, pillow 10.1.0, pytorch 2.4, seaborn 0.13.2, wandb 0.17.6, among others. Our training and evaluations were executed using SLURM on the NYU Langone HPC cluster UltraViolet. We used NVIDIA Cuda 12.1. Our data filtering, data conversion, and training code will be publicly released on GitHub (<https://github.com/nyuolab/>) upon publication of this work. The few-shot examples used in the conversion pipelines will also be omitted as they use excerpts from the *Neurosurgery Publications* materials.

3.3 Acknowledgments

E.K.O. is supported by the National Cancer Institute's Early Surgeon Scientist Program (3P30CA016087-41S1) and the W.M. Keck Foundation. E.K.O. reports consulting with Sofinnova Partners and Google, income from Merck & Co. and Mirati Therapeutics, and equity in Artisight. R.F., T.C.H., and E.K.O. are editorial board members of *Neurosurgery Publications*. D.K. is the editor in chief of *Neurosurgery Publications*. We appreciate the informal input from mentors, colleagues, and lab members of OLAB and Leuthardt Lab not individually acknowledged. We thank Michael Constantino, Ali Siavosh-Haghighi, Kevin Yie, and the rest of the NYU Langone High-Performance Computing (HPC) Team, who supported the computing resources fundamental to our work. Lastly, we thank the NYULH Predictive Analytics Unit for their teamwork and collaboration in making AI technologies a reality at NYULH. We also want to thank the *Congress of Neurological Surgeons* and Wolters Kluwer who run and publish *Neurosurgery Publications*, respectively. We would also like to thank the Managing Editor of *Neurosurgery Publications*, Brandon Fiedor, for his tireless work in promoting medical and scientific scholarship.

3.4 Contributions

E.K.O. conceptualized and supervised the project. A.A., D. Kurland, and K.S. collected journal publication data. A.A. and J.S. extracted, processed, filtered, and organized the data. J.S. developed the front-end and prompting for the graphical abstract-generation pipeline. R.F., T.H., and E.K.O. evaluated generated graphical abstracts. B.D. handled data embedding, mapping, and visualizations. A.A. developed the data conversion pipeline. A.A. and S.S. created forms for human evaluation of the multiple-choice questions. A.S., D. Kurland, C.O., A.V., S.N., E.T.H., I.L., D.L., P.R., L.S., and D. Kondziolka manually evaluated the questions. A.A. developed and trained the models. J.S. built the model evaluation suite. A.A., J.S., and E.K.O. conducted benchmarking and ablations, benchmarking. J.S. and E.K.O. developed the randomized control trial (RCT) user interface and web stack. A.S., C.O., A.V., S.N., A.L., A.P., C.L., I.L., D.O., D.K., and E.K.O. facilitated clinician onboarding to the RCT interface and provided patient data. A.S. and S.F. retrospectively assessed the final diagnoses. A.A. and E.K.O. performed statistical analyses of the RCT data. A.A., D.A.A., K.S., and E.K.O. designed the manuscript figures. A.A. and E.K.O. drafted the manuscript, with all authors contributing to revisions and final edits.

Extended data

Quality of Life After Poor-Grade Aneurysmal Subarachnoid Hemorrhage

Objectives

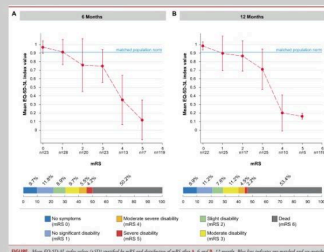
To provide prospective quality of life (QoL) data on survivors of poor-grade aneurysmal subarachnoid hemorrhage (aSAH) to aid clinical decision making and counseling of relatives.

Background

Poor-grade aneurysmal subarachnoid hemorrhage is associated with high mortality and poor disability outcome. Data on quality of life among survivors are scarce because patients with poor-grade aSAH are underrepresented in clinical studies reporting on QoL after aSAH.

Methods

A prospective observational multicenter study was conducted in patients with poor-grade aSAH. Data was collected during structured telephone interviews 6 and 12 months after ictus. QoL was measured using the EuroQoL-5 Dimensions-3 Levels questionnaire, with 0 representing death and 1 representing perfect health. Disability outcome was measured with the modified Rankin Scale.



Mean EQ-5D-3L index values (+SD) stratified by mRS and distribution of mRS after 6 and 12 months. Blue line indicates age-matched and sex-matched population norm (0.91 + 0.04).

Results

Of 250 enrolled patients, 237 were included in the 6-month analysis and 223 in the 12-month analysis. After 6 months, 118 (49.8%) patients were alive, with 80.5% reaching favorable outcomes and mean EQ-5D-3L index values of 0.85. After 12 months, 104 (46.6%) patients were alive, with 85.6% achieving favorable outcomes and mean EQ-5D-3L index values of 0.86.

Discussion

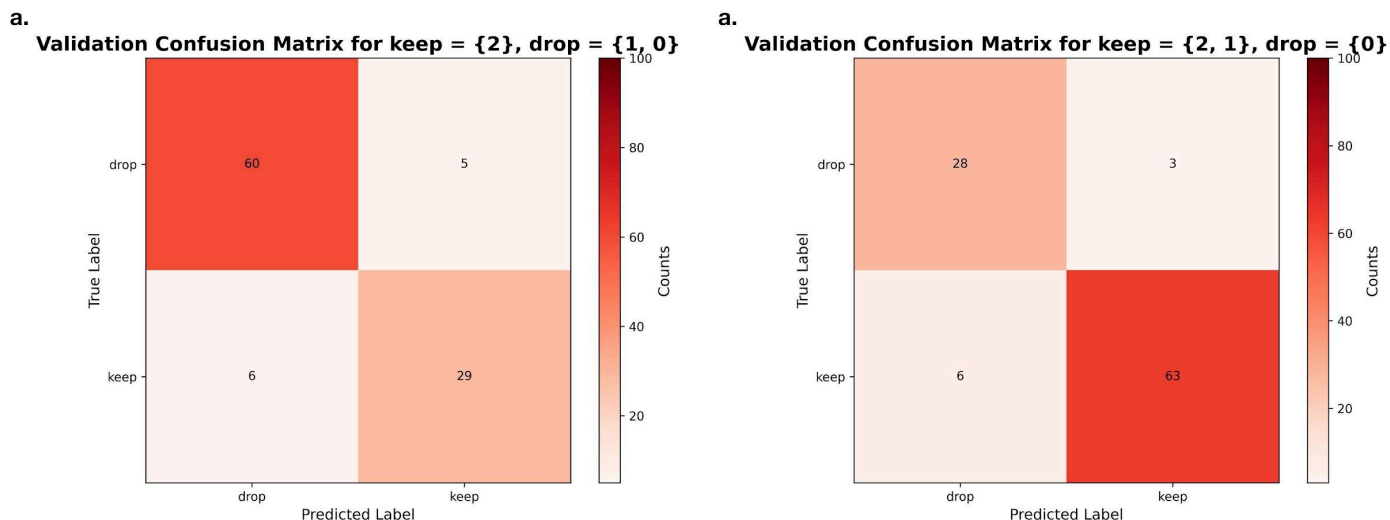
Despite high initial mortality, approximately 80% of poor-grade aSAH survivors have a favorable outcome, can return home, and have good QoL. About 20% reported no restriction in any health domain. Patients with favorable outcomes showed EQ-5D-3L index values close to the matched population norm, indicating reasonably good outcomes after such a potentially devastating disease.

Conclusion

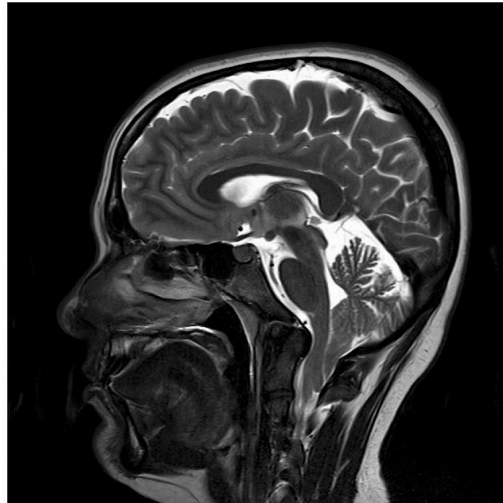
Despite high initial mortality, the proportion of poor-grade aSAH survivors with good QoL is reasonably large. Only a minority of survivors reports poor QoL and requires permanent care.



Extended Data Figure 1. Automatically generated graphical abstract example. An abstract generated from *Magill et al. International Tuberculoma Sellae Meningioma Study: Preoperative Grading Scale to Predict Outcomes and Propensity-Matched Outcomes by Endonasal Versus Transcranial Approach*³¹ via parsing extracted figures and texts with Clade Sonnet-3.5.



Extended Data Figure 2. Dataset filtering. Validation confusion matrices for the image content classification system. The classifier, based on ResNet-50 feature extraction and a linear classifier trained on 400 manually annotated images, was used to filter figures for the differential diagnosis dataset (Class 2 only) and the multiple-choice dataset (Classes 1 and 2). Confusion matrices demonstrate validation performance on the held out 100 manually labeled images. **a.** Performance of the classifier when retaining Class 2 images (medical imaging: CT, MRI, X-ray, angiography) and filtering out Classes 1 (clinical visuals: surgical fields, microscopy, anatomical drawings) and 0 (technical content: flowcharts, survival curves, tables). Used to create the differential diagnosis dataset. **b.** Classifier performance when retaining Classes 1 and 2 combined while filtering out Class 0. Used to create the multiple choice dataset.



CAPTION

Figure 3. A case of a patient with Chiari 1.5 malformation. A 30 year old female patient presenting with headache and dizziness. No other complaints and no trauma. A sagittal T2 MRI showing a herniation of the cerebellar tonsils through the foramen magnum (about 2.0 cm), including bulb and obex herniation, associated with retroflexion of the odontoid process, with a compressive effect on the bulb, which is reduced in anteroposterior thickness. Case courtesy of Rodrigo Dias Duarte, Radiopaedia.org, rID: 50409

IN-TEXT MENTION

Chiari 1.5 malformation, or bulbar variant of Chiari 1 malformation, is a term used in the literature to describe the combination of cerebellar tonsillar herniation (Chiari 1) along with caudal herniation of some portion of the brainstem (often obex of the medulla oblongata) through the foramen magnum. It is believed that when congenital, it is the progression of Chiari 1 malformation. (See Fig. 3)

CONVERSATION

User: What type of MRI is shown in the image?

Assistant: The image is a sagittal T2-weighted MRI.

User: What condition does the patient have?

Assistant: The patient has Chiari 1.5 malformation.

User: What is herniated through the foramen magnum?

Assistant: The cerebellar tonsils, as well as the bulb and obex, are herniated through the foramen magnum.

User: Is there any effect on the medulla oblongata?

Assistant: Yes, there is a compressive effect on the medulla oblongata (bulb), which is reduced in anteroposterior thickness.

User: What additional structural change is observed?

Assistant: There is retroflexion of the odontoid process noted.

DIFFERENTIAL DIAGNOSIS

One-Liner: A 30-year-old female presents with headache and dizziness, found to have cerebellar tonsillar and brainstem herniation on imaging.

Possible Diagnoses:

- Chiari Malformation Type 1.5
- Basilar Invagination
- Hydrocephalus
- Syringomyelia
- Arnold–Chiari Malformation

MC QUESTION

Question:

A 30-year-old female presents with headaches and dizziness. An MRI reveals herniation of the cerebellar tonsils and a portion of the brainstem through the foramen magnum, along with retroflexion of the odontoid process. What is the most appropriate surgical approach for treating the compressive symptoms associated with this malformation?

- A. Suboccipital decompression with duraplasty
- B. Endoscopic third ventriculostomy
- C. Posterior fossa tumor resection
- D. Cervical laminectomy
- E. Anterior cervical discectomy and fusion

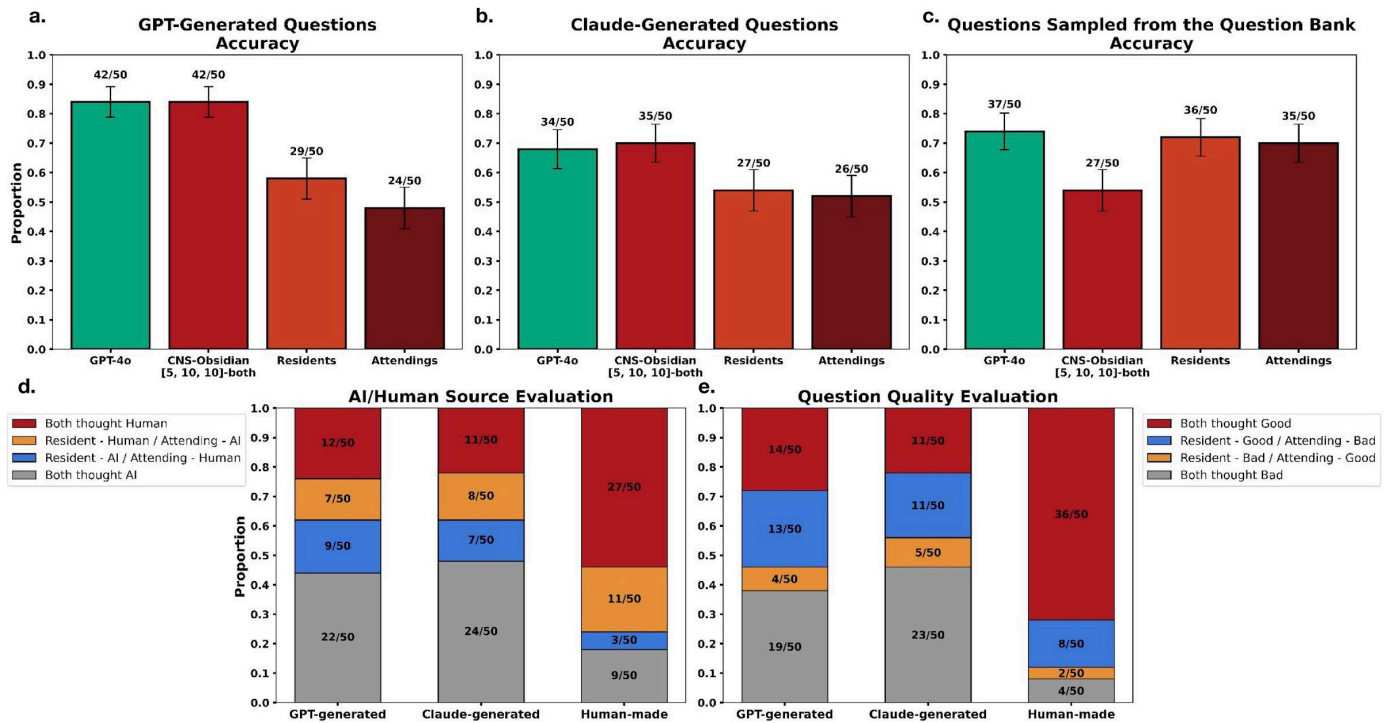
Correct Answer:

A. Suboccipital decompression with duraplasty

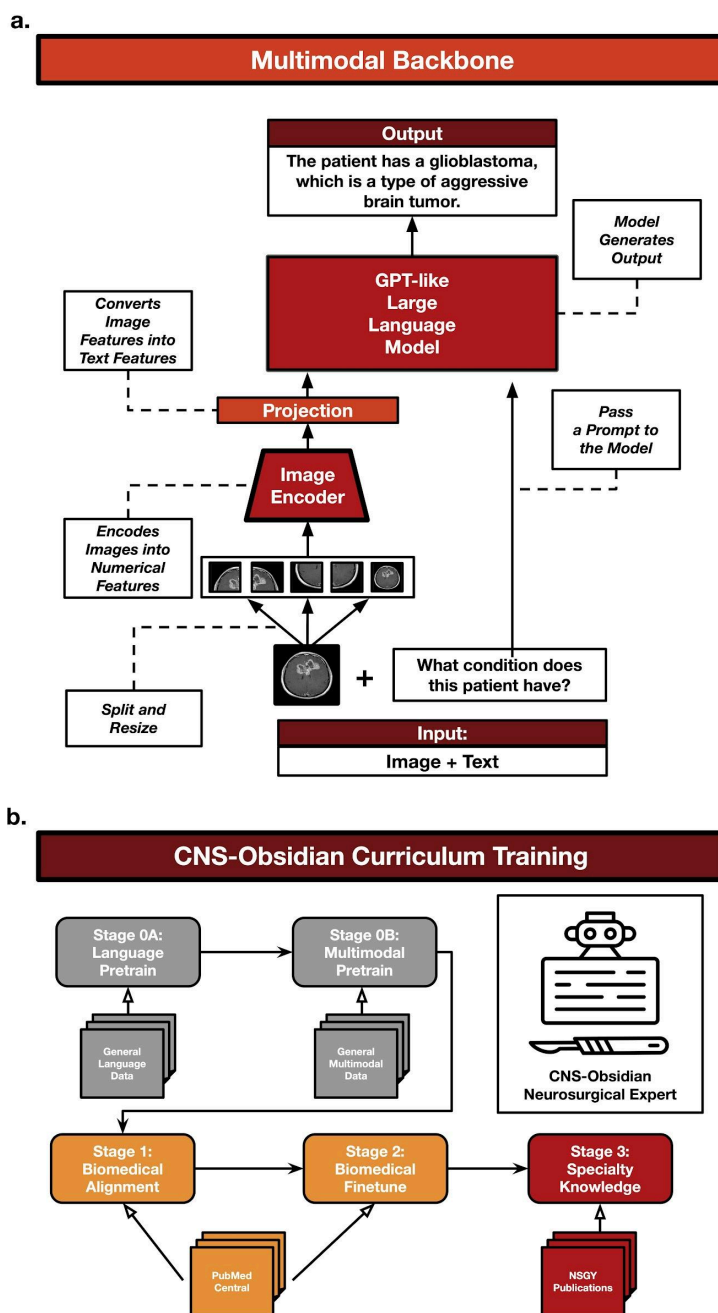
Discussion:

The imaging and clinical presentation are consistent with Chiari 1.5 malformation, characterized by herniation of the cerebellar tonsils and caudal herniation of the brainstem through the foramen magnum. This can lead to compression of posterior fossa structures, causing symptoms like headache and dizziness. The standard surgical treatment for symptomatic Chiari malformation (including Chiari 1.5) is suboccipital decompression with duraplasty (Option A). This procedure involves removing a portion of the occipital bone and sometimes part of the first cervical vertebra (C1 laminectomy) to relieve pressure and restore normal cerebrospinal fluid flow. A duraplasty may be performed to expand the dura and further alleviate compression. Options B, C, D, and E do not address the core issue of posterior fossa compression caused by Chiari malformation. Endoscopic third ventriculostomy (B) is used mainly for obstructive hydrocephalus. Posterior fossa tumor resection (C) is unrelated as there is no indication of a tumor. Cervical laminectomy (D) could be used if there were additional spinal cord compression at other cervical spine levels. Anterior cervical discectomy and fusion (E) treats cervical spine issues unrelated to Chiari malformation. Therefore, the best approach here is suboccipital decompression with duraplasty to alleviate the compression of neural structures.

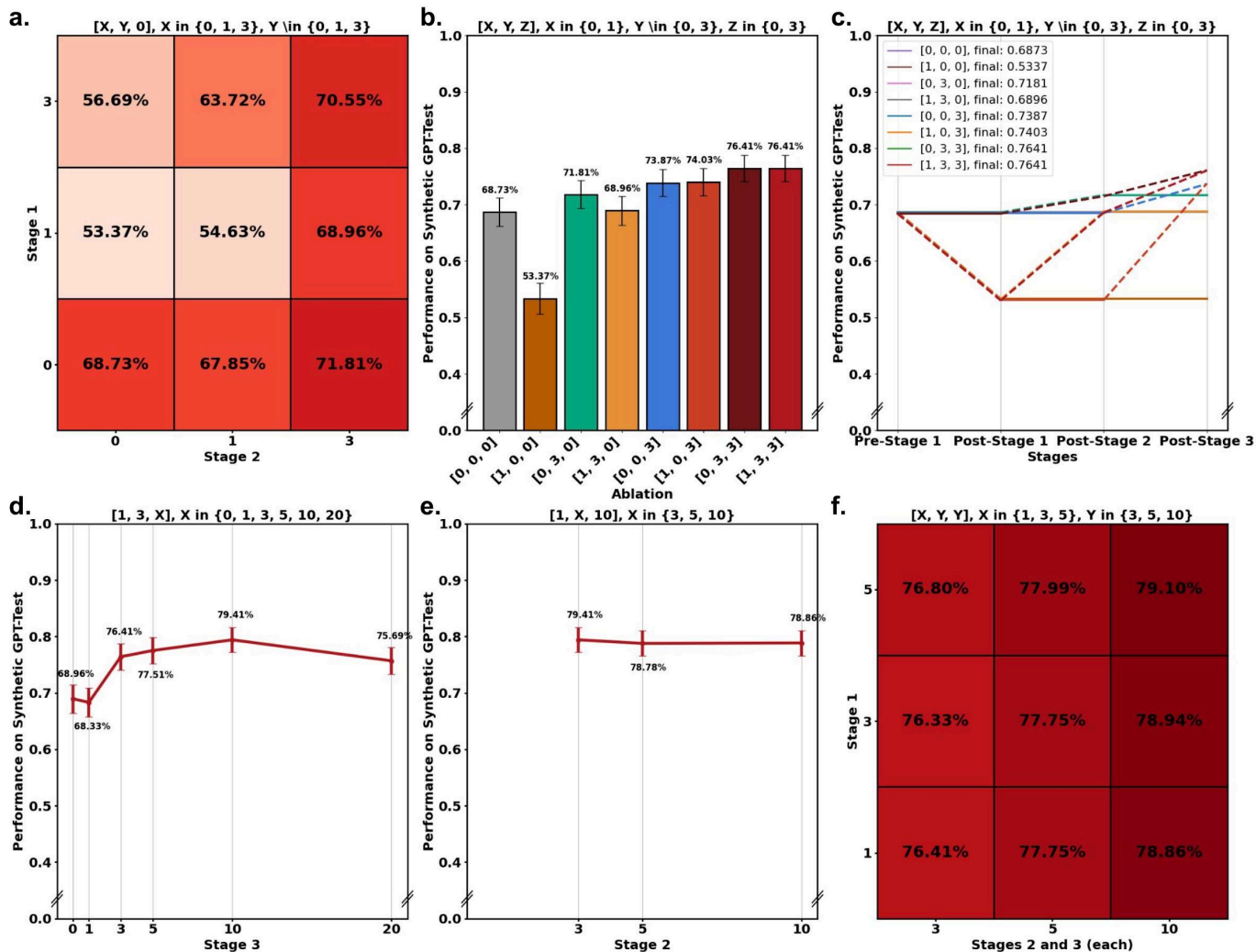
Extended Data Figure 3. Knowledge translation pipeline demonstrated through conversion of neurosurgical data into training datasets. The example illustrates the automated conversion of specialized knowledge (figure, caption, in-text mention) into three distinct data formats: 1) natural instructional dialogue between user and assistant, 2) clinical vignette with multiple-choice options and detailed explanation, and 3) concise one-liner with prioritized differential diagnoses. The pipeline employs large language models (GPT-4o here) with few-shot in-context learning (four examples for each task randomly selected from pools of 10) to generate consistently formatted outputs while preserving diagnostic accuracy and educational value. Image: case courtesy of Rodrigo Dias Duarte, Radiopaedia.org, rID: 50409. Caption and in-text mention written based on the case information provided on Radiopaedia.org.



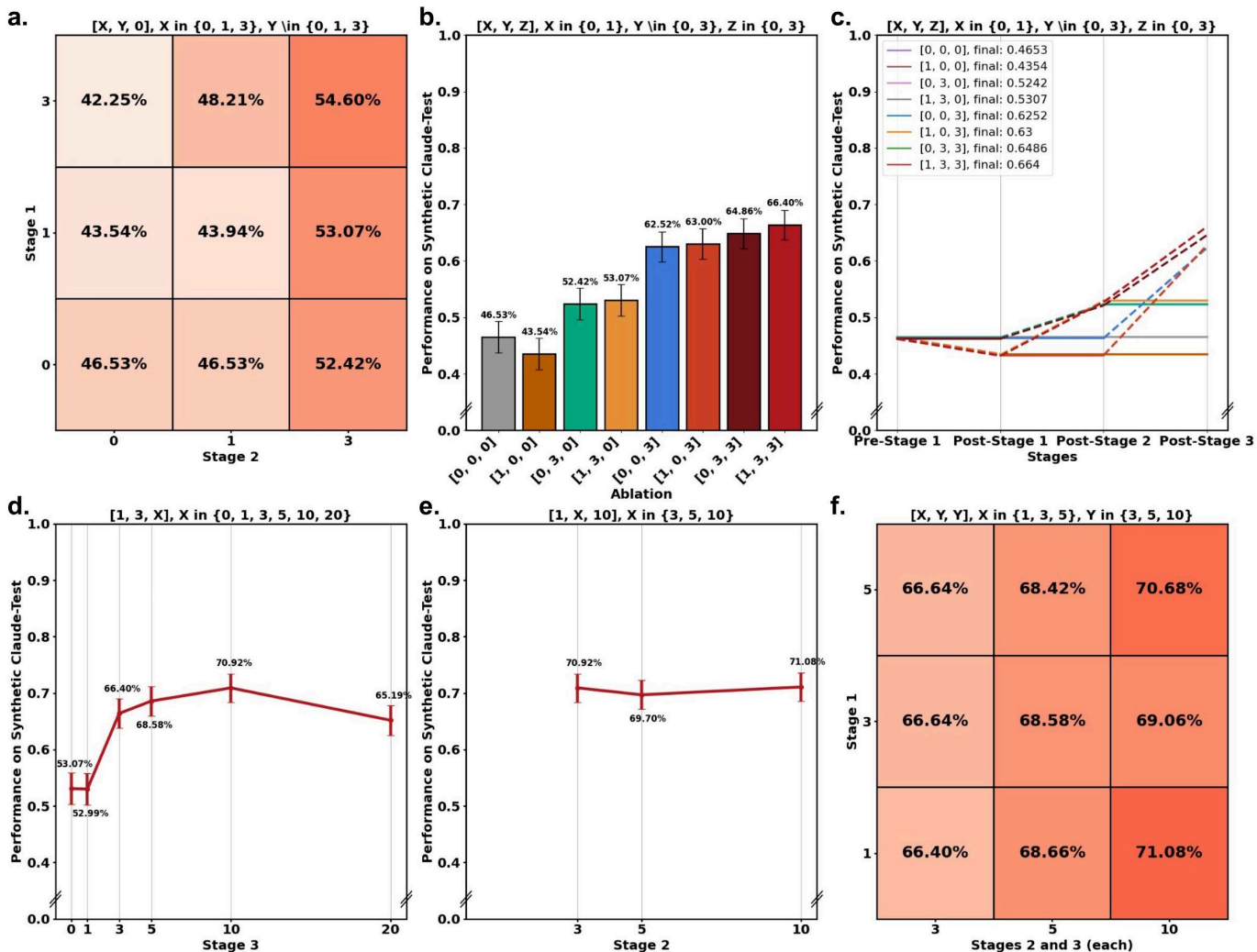
Extended Data Figure 4. Multiple choice human evaluation. Thirty-question forms (10 GPT-generated, 10 Claude-generated, 10 board examination question bank - Self-Assessment of Neurological Surgery, SANS) were distributed to residents and attendings to evaluate accuracy and compare human performance with VLMs (GPT-4o and CNS-Obsidian). **a-c.** Accuracy: VLM and human performance on GPT-generated, Claude-generated MCQs, and self-assessment question samples. The GPT-generated MCQs and Claude-generated MCQs consist of questions excluded from the CNS-Obsidian training data. **d.** Human Identification of Question Origin: Participants guessed whether questions were from the self-assessment bank or AI-generated. SANS questions were more often perceived as human-made than GPT-generated (residents, $p = 0.0002$; attendings, $p = 0.1091$) and Claude-generated (residents, $p = 0.0002$; attendings, $p = 0.0272$) questions for both groups. Notably, 54% of AI-generated questions misled at least one evaluator, and 23% misled both. **e.** Question Quality Ratings: Evaluators rated questions as suitable for neurosurgery board exams. SANS questions outperformed GPT-generated (residents, $p < 10^{-5}$; attendings, $p = 0.0001$) and Claude-generated (residents and attendings, $p < 10^{-5}$) questions. Pooled together SANS outperformed AI-generated questions if measured by consensus of the reviewers (requiring both evaluators to mark the question as good, $p < 10^{-7}$).



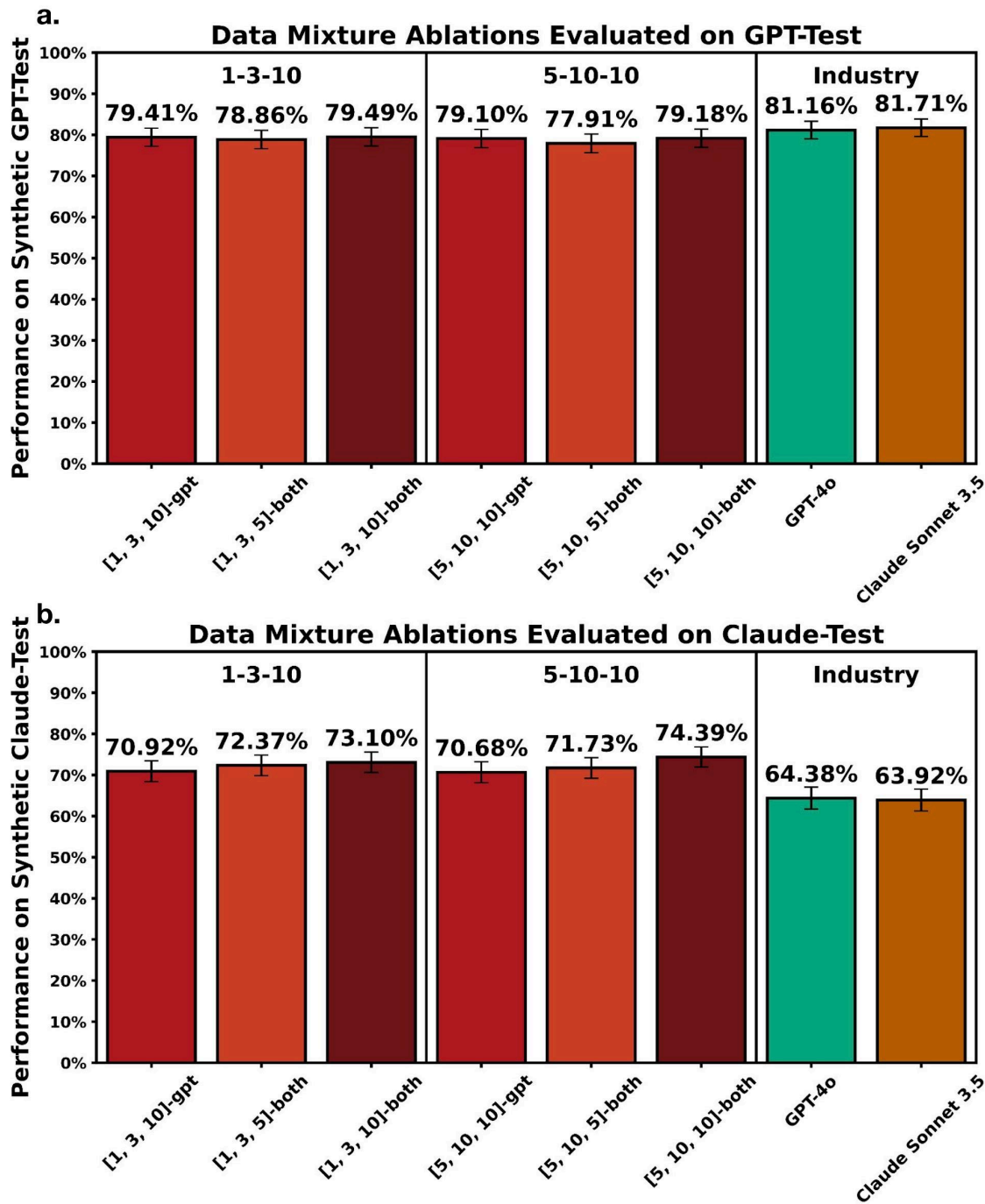
Extended Data Figure 5. Training a specialty vision-language model: **a**, LLaVA-Next is a vision-language model that combines two modalities by slicing the high-resolution image into small patches and embedding them together with a resized full image. It then projects the visual features into the text space, and uses a pre-trained autoregressive model to generate output conditioned on both the image and the prompt. **b**, A specialist model is trained in a stages, beginning with general language and multimodal pretraining (Stages 0A and 0B), followed by general medical alignment and finetuning (Stages 1 and 2), and culminating in specialty knowledge integration (Stage 3) using NeuroPubs. This curriculum-based approach was used to create CNS-Obsidian, a neurosurgical expert system capable of interpreting medical imaging and providing specialized diagnostic assessments.



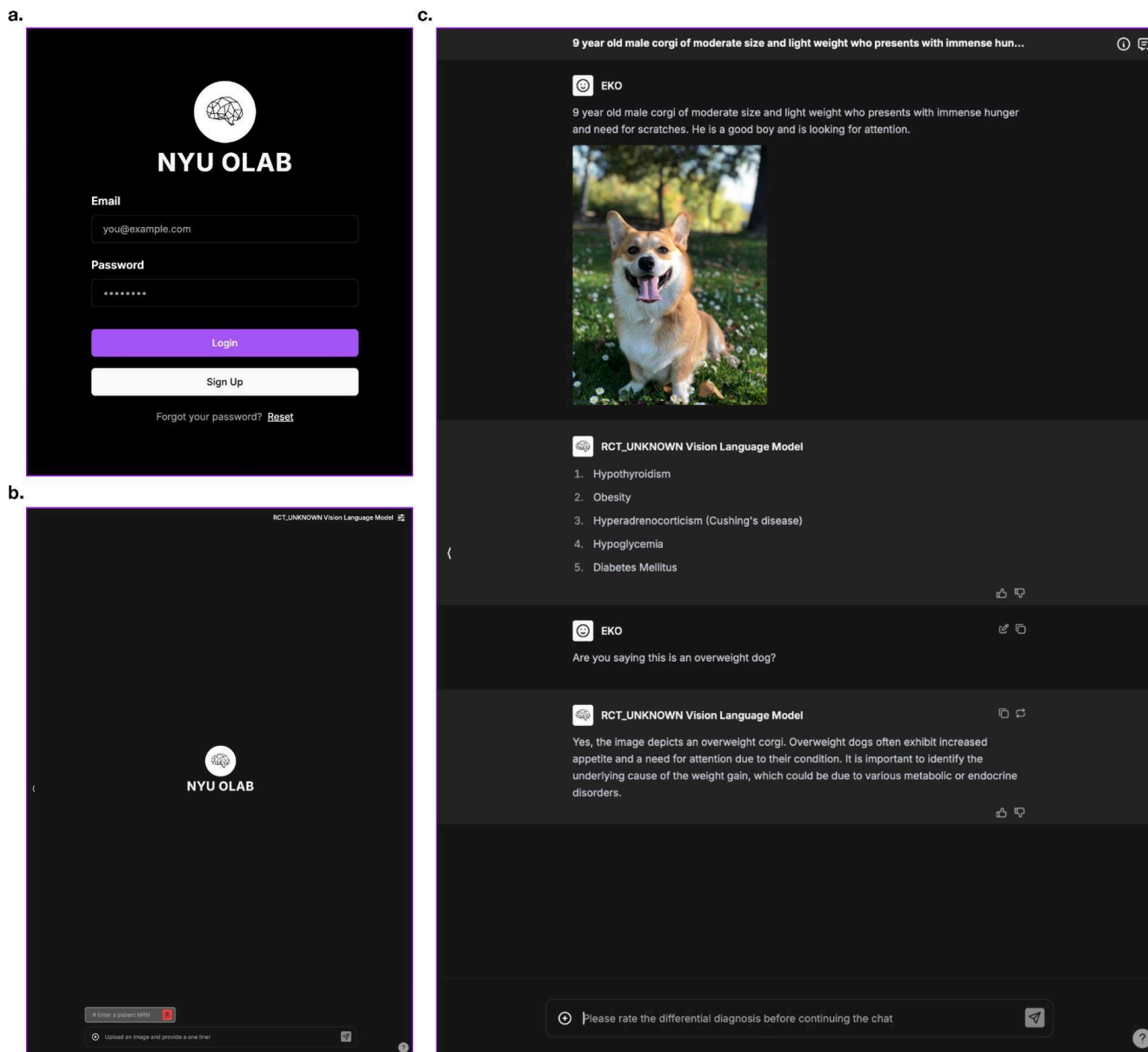
Extended Data Figure 6. Ablation studies of three-stage training using GPT-generated evaluations. Configuration $[X, Y, Z]$ denotes number of epochs in Stages 1, 2, and 3. **a.** Impact of Stage 1 (alignment) and Stage 2 (general fine-tuning) epochs on model accuracy using GPT generated MCQs dataset ($n=1,282$), with Stage 3 fixed at 0. Darker red indicates higher accuracy. Baseline $[0, 0, 0]$ achieves 68.73%. Alignment-only training shows performance degradation. **b.** Performance comparison across configurations demonstrating each training stage's contribution. Error bars represent standard error. The full three-stage model $[1, 3, 3]$ achieves 76.41% accuracy, with Stage 3 contributing the largest improvement (+7.45%, $p < 0.0001$). **c.** Temporal evolution of model performance across training stages for different configurations. Solid lines represent measurements, dashed lines show interpolated trajectories. **d.** Optimization of Stage 3 (task-specific fine-tuning) duration using configuration $[1, 3, X]$, where X varies from 0 to 20 epochs. Performance exhibits monotonic improvement until peaking at $X = 10$ epochs (79.48%). **e.** Impact of Stage 2 duration on model performance using configuration $[1, X, 10]$, where X varies from 3 to 10 epochs. Performance remains stable across durations, $[1, 3, 10]$ achieving optimal performance (79.41%) on GPT generated MCQs and selected as one of final configuration candidates. **f.** Joint optimization of Stage 1 and Stage 2/3 durations (configurations $[X, Y, Y]$). Longer fine-tuning stages show performance improvements. $[5, 10, 10]$ selected as one of the final configurations.



Extended Data Figure 7. Ablation studies of three-stage training using Claude-generated evaluations. Configuration $[X, Y, Z]$ denotes number of epochs in Stages 1, 2, and 3. **a.** Impact of Stage 1 (alignment) and Stage 2 (general fine-tuning) epochs on model accuracy using Claude generated MCQs dataset ($n=1,239$), with Stage 3 fixed at 0. Darker red indicates higher accuracy. Baseline $[0, 0, 0]$ achieves 46.53%. Alignment-only training $[1, 0, 0]$ decreases performance to 43.54%. **b.** Performance comparison across configurations showing each stage's contribution. Error bars represent standard error. The full three-stage model $[1, 3, 3]$ shows substantial improvement, with Stage 3 providing the largest gain (+13.33%, $p < 10^{-12}$). **c.** Temporal evolution of model performance across training stages. Solid lines represent measurements, dashed lines show interpolated trajectories. **d.** Optimization of Stage 3 duration using configuration $[1, 3, X]$. Performance peaks at $X = 10$ epochs (70.92%) before plateauing. **e.** Effect of Stage 2 duration $[1, X, 10]$. Performance remains stable, with $[1, 10, 10]$ achieving slightly better results (71.08%, $p = 0.9647$). **f.** Joint optimization of Stage 1 and Stage 2/3 durations (configurations $[X, Y, Y]$). Longer training shows improvements, leading to selection of $[5, 10, 10]$ for final evaluation using both datasets.




Extended Data Figure 8. Ablation experiments for data mixtures. **a.** Performance on GPT generated MCQs ($n=1,282$) comparing models trained on GPT-generated data only (*-gpt*) versus both data sources (*-both*). Two base configurations $[1, 3, 10]$ and $[5, 10, 10]$ were each evaluated under two constraints when using both datasets: compute-matched (halved epochs) and epoch-matched (doubled compute due to doubled dataset). Including Claude-generated data showed no improvement over GPT-only training ($p = 1.000$ for $[5, 10, 10]$ -*gpt* vs. $[5, 10, 10]$ -*both*). Models approach industry standard **b.** Performance on Claude generated MCQs ($n=1,239$). Epoch-matched training on both datasets shows significant improvement ($p = 0.0427$), with $[5, 10, 10]$ -*both* reaching 74.39% compared to baseline Claude Sonnet 3.5, 63.92%. In both evaluations, epoch-matched consistently outperforms compute-matched training. Error bars represent standard error.



Extended Data Figure 9. Randomized controlled trial user interface. **a.** The landing login interface. All participants had individual accounts with stored chat histories. Access was manually curated by the team. **b.** Post-login, the participants are directly forwarded to the chatbot interface which is designed to mimic the typical chatbot interfaces, but enhanced with randomized back-end, a patient MRN field, and an ability to submit an image, including via intuitive “drag-and-drop”. **c.** An example interaction with the model. The users can provide binary feedback for individual messages using “upvote” and “downvote” buttons. The model interacted with for this chat is CNS-Obsidian, but the participants are blinded to this information.

😊

This is a 50 year old man presenting to ER with acute paraplegia. He's on warfarin.



RCT_UNKNOWN Vision Language Model

1. Spinal epidural hematoma
2. Spinal cord compression
3. Spinal arteriovenous malformation
4. Intramedullary spinal tumor
5. Spinal abscess

👍 🗨️

😊

Which of these is it most likely?

RCT_UNKNOWN Vision Language Model

Given the patient's presentation of acute paraplegia and the imaging findings of a hyperintense lesion in the spinal cord on T2-weighted MRI, the most likely diagnosis is a spinal epidural hematoma. This condition is characterized by rapid onset of symptoms due to the acute compression of the spinal cord by a hematoma. The patient's use of warfarin further supports this diagnosis as it can predispose to spontaneous bleeding. Other conditions like spinal cord compression, spinal arteriovenous malformation, intramedullary spinal tumor, and spinal abscess may present similarly but are less likely given the acute presentation and the use of anticoagulants. A detailed clinical history, imaging findings, and neurological examination will help confirm the diagnosis and guide management.

👍 🗨️

😊

What is the treatment?

RCT_UNKNOWN Vision Language Model

The treatment for a spinal epidural hematoma typically involves urgent surgical intervention to evacuate the hematoma and relieve the compression on the spinal cord. This is to prevent further neurological deterioration and to restore neurological function. Immediate discontinuation of anticoagulant therapy such as warfarin is also necessary to prevent further bleeding. Postoperatively, careful monitoring of neurological status, pain management, and rehabilitation are crucial for optimal recovery. Management of the underlying cause of the bleeding, such as stopping anticoagulation or addressing a bleeding disorder, is also important.

👍 🗨️

⊕ Please rate the differential diagnosis before continuing the chat 🗨️

Extended Data Figure 10. An example patient submitted to the study interface. Identifying details anonymized. The model interacted with is CNS-Obsidian-base (version actually used in the trial). For more examples of a base and final model see **Supplementary Video 1** and **Supplementary Video 2**, respectively.

References

1. Senior, A. W. *et al.* Improved protein structure prediction using potentials from deep learning. *Nature* **577**, 706–710 (2020).
2. Lu, C. *et al.* The AI Scientist: Towards fully automated open-ended scientific discovery. *arXiv [cs.AI]* (2024).
3. Bagenal, J. Generative artificial intelligence and scientific publishing: urgent questions, difficult answers. *Lancet* **403**, 1118–1120 (2024).
4. Conroy, G. How ChatGPT and other AI tools could disrupt scientific publishing. *Nature* **622**, 234–236 (2023).
5. Neurosurgery. <https://journals.lww.com/neurosurgery/pages/default.aspx>.
6. Smith, E. The Edwin Smith Surgical Papyrus. (1930).
7. History of Philosophical Transactions.
<https://royalsociety.org/journals/publishing-activities/publishing350/history-philosophical-transactions/>.
8. Bubeck, S. *et al.* Sparks of Artificial General Intelligence: Early experiments with GPT-4. *arXiv [cs.CL]* (2023).
9. Alayrac, J.-B. *et al.* Flamingo: A visual language model for few-shot learning.
<https://storage.googleapis.com/deepmind-media/DeepMind.com/Blog/tackling-multiple-tasks-with-a-single-visual-language-model/flamingo.pdf>.
10. Gunasekar, S. *et al.* Textbooks are all you need. *arXiv [cs.CL]* (2023).
11. Cheng, J. *et al.* Accurate proteome-wide missense variant effect prediction with AlphaMissense. *Science* **0**, eadg7492.
12. Berman, H. M. *et al.* The Protein Data Bank. *Nucleic Acids Res* **28**, 235–242 (2000).
13. Lek, M. *et al.* Analysis of protein-coding genetic variation in 60,706 humans. *Nature* **536**, 285–291 (2016).
14. Luo, R. *et al.* BioGPT: generative pre-trained transformer for biomedical text generation and mining. *Brief. Bioinform.* **23**, (2022).
15. Li, C. *et al.* LLaVA-Med: Training a Large Language-and-Vision Assistant for Biomedicine in One Day. *arXiv [cs.CV]* (2023).
16. Huang, Z., Bianchi, F., Yuksekgonul, M., Montine, T. J. & Zou, J. A visual-language foundation model for pathology image analysis using medical Twitter. *Nat. Med.* (2023) doi:10.1038/s41591-023-02504-3.
17. Zhang, H. *et al.* LLaVA-Grounding: Grounded Visual Chat with Large Multimodal Models. *arXiv [cs.CV]* (2023).
18. Nori, H., King, N., McKinney, S. M., Carignan, D. & Horvitz, E. Capabilities of GPT-4 on Medical Challenge Problems. *arXiv [cs.CL]* (2023).
19. Deng, C., Zhao, Y., Tang, X., Gerstein, M. & Cohan, A. Investigating Data Contamination in Modern Benchmarks for Large Language Models. (2023).
20. McDuff, D. *et al.* Towards Accurate Differential Diagnosis with Large Language Models. *arXiv [cs.CY]* (2023).
21. Tu, T. *et al.* Towards Conversational Diagnostic AI. *arXiv [cs.AI]* (2024).
22. Dai, W. *et al.* NVLM: Open Frontier-Class Multimodal LLMs. *arXiv [cs.CL]* (2024).
23. Triantafyllopoulos, L. *et al.* Evaluating the interactions of Medical Doctors with chatbots based on large language models: Insights from a nationwide study in the Greek healthcare sector using ChatGPT. *Comput. Human Behav.* **161**, 108404 (2024).
24. Thulke, D., Daheim, N., Dugast, C. & Ney, H. Efficient Retrieval Augmented Generation from Unstructured Knowledge for

Task-Oriented Dialog. *arXiv [cs.CL]* (2021).

25. Vishwanath, K., Stryker, J., Alyakin, A., Alber, D. A. & Oermann, E. K. MedMobile: A mobile-sized language model with expert-level clinical capabilities. *arXiv [cs.CL]* (2024).
26. Blecher, L., Cucurull, G., Scialom, T. & Stojnic, R. Nougat: Neural Optical Understanding for Academic Documents. *arXiv [cs.LG]* (2023).
27. He, K., Zhang, X., Ren, S. & Sun, J. Deep residual learning for image recognition. *Proc. IEEE Comput. Soc. Conf. Comput. Vis. Pattern Recognit.* 770–778 (2015).
28. Nussbaum, Z., Duderstadt, B. & Mulyar, A. Nomic Embed Vision: Expanding the Latent Space. *arXiv [cs.CV]* (2024).
29. van der Maaten, L. & Hinton, G. Visualizing Data using t-SNE. *J. Mach. Learn. Res.* **9**, 2579–2605 (2008).
30. Campello, R. J. G. B., Moulavi, D. & Sander, J. Density-based clustering based on hierarchical density estimates. in *Advances in Knowledge Discovery and Data Mining* 160–172 (Springer Berlin Heidelberg, Berlin, Heidelberg, 2013).
31. Magill, S. T. *et al.* International tuberculoma sellae meningioma study: Preoperative grading scale to predict outcomes and propensity-matched outcomes by endonasal versus transcranial approach. *Neurosurgery* **93**, 1271–1284 (2023).